Extrusion and Microfluidic-Based Bioprinting to Fabricate Biomimetic Tissues and Organs

Elham Davoodi, Einollah Sarikhani, Hossein Montazerian, Samad Ahadian, Marco Costantini, Wojciech Swieszkowski, Stephanie Michelle Willerth, Konrad Walus, Mohammad Mofidfar, Ehsan Toyserkani, Ali Khademhosseini & Nureddin Ashammakhi

May 2020

ADVANCED MATERIALS TECHNOLOGIES
www.advmattechnol.de

Extrusion and Microfluidic-Based Bioprinting to Fabricate Biomimetic Tissues and Organs

Elham Davoodi, Einollah Sarikhani, Hossein Montazerian, Samad Ahadian, Marco Costantini, Wojciech Swieszkowski, Stephanie Michelle Willerth, Konrad Walus, Mohammad Mofidfar, Ehsan Toyserkani, Ali Khademhosseini, and Nureddin Ashammakhi**

Next generation engineered tissue constructs with complex and ordered architectures aim to better mimic the native tissue structures, largely due to advances in 3D bioprinting techniques. Extrusion bioprinting has drawn tremendous attention due to its widespread availability, cost-effectiveness, simplicity, and its facile and rapid processing. However, poor printing resolution and low speed have limited its fidelity and clinical implementation. To circumvent the downsides associated with extrusion printing, microfluidic technologies are increasingly being implemented in 3D bioprinting for engineering living constructs. These technologies enable biofabrication of heterogeneous biomimetic structures made of different types of cells, biomaterials, and biomolecules. Microfluiding bioprinting technology enables highly controlled fabrication of 3D constructs in high resolutions and it has been shown to be useful for building tubular structures and vascularized constructs, which may promote the survival and integration of implanted engineered tissues. Although this field is currently in its early development and the number of bioprinted implants is limited, it is envisioned that it will have a major impact on the production of customized clinical-grade tissue constructs. Further studies are, however, needed to fully demonstrate the effectiveness of the technology in the lab and its translation to the clinic.

1. Introduction

The increasing demand for tissue grafts[1–3] and organ repair and regeneration[4,5] has led to the development of 3D bioprinting as a new modality for fabricating viable tissue constructs.[6–11] 3D bioprinting is an additive manufacturing process where cell-laden structures are laid down in a layer-by-layer fashion to obtain 3D tissue structures.[12] To achieve this, various types of 3D bioprinting techniques have been developed, such as microextrusion,[13–15] inkjet,[16–18] laser-assisted,[19–21] and stereolithographic (SLA) printing methods.[22–24]

Microextrusion bioprinting is one of the most common types of additive manufacturing techniques,[25] in which cell-laden bioinks are dispensed through a nozzle or syringe to form filaments, fibers, or droplets and make layer-by-layer cell-laden scaffolds.[26] Microextrusion relies on the application of force to dispense the biomaterial from the syringe or nozzle.[27]

E. Davoodi, Prof. E. Toyserkani
Department of Mechanical and Mechatronics Engineering
University of Waterloo
Waterloo, ON N2L 3G1, Canada

E. Davoodi, E. Sarikhani, H. Montazerian, Dr. S. Ahadian, Prof. A. Khademhosseini, Prof. N. Ashammakhi
Center for Minimally Invasive Therapeutics (C-MIT)
University of California
Los Angeles, CA 90095, USA
E-mail: khademh@terasaki.org; n.ashammakhi@ucla.edu

The ORCID identification number(s) for the author(s) of this article can be found under https://doi.org/10.1002/admt.201901044.

DOI: 10.1002/admt.201901044

E. Davoodi, E. Sarikhani, H. Montazerian, Dr. S. Ahadian, Prof. A. Khademhosseini, Prof. N. Ashammakhi
Department of Bioengineering
University of California
Los Angeles, CA 90095, USA

Dr. M. Costantini, Prof. W. Swieszkowski
Biomaterials Group, Materials Design Division, Faculty of Materials Science and Engineering
Warsaw University of Technology
Warsaw 00-661, Poland

Dr. M. Costantini
Institute of Physical Chemistry
Polish Academy of Sciences
Warsaw 01-224, Poland

Prof. S. M. Willerth
Department of Mechanical Engineering, Division of Medical Sciences
University of Victoria
Victoria, BC V8P 5C2, Canada

Dr. K. Walus
Department of Electrical and Computer Engineering
University of British Columbia
Vancouver, BC V6T 1Z4, Canada

Microextrusion bioprinters can print a wide variety of materials with different viscosities.[28] Bioink properties and viscosity play an important role in the resolution and accuracy of printing. However, other parameters, such as printing speed, dispensing pressure or mechanical force, and distance should be taken into an account.[13,26] Microextrusion bioprinting has the advantage of printing constructs with high cell density in a controllable manner under physiological conditions. The diameter of the nozzle is another factor that may significantly govern cell viability. For instance, the viability of bovine aortic endothelial cells encapsulated in collagen for 250 and 90 μm diameter nozzles were found to be 86% and 46%, respectively.[13]

Inkjet printing is considered an important type of printing of living cells as droplets.[29][30] Inkjet-based printers can utilize thermal, electromagnetic, or piezoelectric forces to deposit droplets of a bioink onto a substrate. To control the size of the droplets, parameters, such as ultrasound duration, amplitude, and pulse can be adjusted. Inkjet printers have widely been used due to their relatively low cost, high speed, and convenience. However, the application of this technique compared to other techniques has been limited due to limited cell viability as a result of cell exposure to thermal and mechanical stress, nozzle clogging, and nonuniform droplets.[28,31]

Laser-assisted bioprinting is mostly used for high-resolution patterning of bioinks. In this technique, bioink is projected from a film to the depositing stage by using a laser beam as a driving force to trigger the droplet release. [32–34] A laser pulse evaporates the bioink, creating an expanding bubble followed by jet formation and finally deposition of a droplet onto the receiving substrate. The resolution of this technique can vary with changing parameters, such as viscosity, printing speed, pattern topology, and laser pulse energy.[35,36] One of the main advantages of this method over other types of bioprinting is its high resolution and accuracy of the printed pattern.[34] In addition, cell loading capacity in this method is comparable to microextrusion-based bioprinting method.[37] However, preparing each ribbon for each type of biological agent is time-consuming and challenging in case of printing with multiple cell lines.[38]

SLA is a nozzle-free bioprinting technique in which ink is solidified using an ultraviolet (UV) light or a laser beam over a liquid polymer. In SLA, there is a micromirror array that can selectively adjust the light intensity to polymerize the bioink.[39] SLA printing has high accuracy and precision fabrication that can print light-sensitive bioinks.[40] However, there are some limitations for the use of SLA bioprinting, such as the limited number of biocompatible materials available for the SLA bioprinting, time-consuming UV crosslinking process, which can be harmful to the incorporated biological components.[40,41]

These bioprinting methods have been used to fabricate various types of tissue constructs, such as cardiac,[42–44] vascular,[45–47] muscle,[48–51] and cartilage.[52–55] However, these tissue constructs often fall short of being completely functional after their fabrication. 3D bioprinted constructs should recapitulate as much of the

Dr. M. Mofidfar
Department of Biomedical Engineering
University of Southern California
Los Angeles, CA 90089, USA

Prof. A. Khademhosseini
Department of Chemical and Biomolecular Engineering
University of California
Los Angeles, CA 90095, USA

Prof. A. Khademhosseini
Terasaki Institute for Biomedical Innovation
Los Angeles, CA 90024, USA

Prof. A. Khademhosseini, Prof. N. Ashammakhi
Department of Radiological Sciences
University of California
Los Angeles, CA 90095, USA

Elham Davoodi is currently a Ph.D. candidate at the Mechanical and Mechatronics department of University of Waterloo. She received her M.Sc. in mechanical engineering at Texas Tech university in 2017. Her research interests include additive manufacturing technologies and flexible electronics for health monitoring wearable devices.

Ali Khademhosseini is the Distinguished Professor and Founding Director of Terasaki Institute for Biomedical Innovation. He was previously a professor of Medicine at Harvard Medical School and Bioengineering at UCLA. He is recognized as a leader in combining micro- and nano-engineering approaches with advanced biomaterials for regenerative medicine applications.

Nureddin Ashammakhi is an Associate Director of the Center for Minimally Invasive Therapeutics at UCLA, leading translational research in regenerative therapy. He has extensive experience with biodegradable implants, drug release, and nanofiber-based scaffolds. Currently, he is working on 3D bioprinting and organ-on-a-chip models for regenerative and personalized medicine. He was previously a professor of Biomaterials Technology in Tampere University of Technology, Finland, Chair of Regenerative Medicine in Keele University, UK and adjunct professor in Oulu University, Finland before he joined University of California - Los Angeles first as a visiting professor (scholar) and then as an adjunct professor.

native tissue function as possible. It should be noted that native tissues consist of matrices comprised of various phases of fibrous and fluid materials.[56–58] These tissues also have different types of cells that are organized in specific patterns to form structures, such as vessels, lymphatics, nerves, parenchymal, and stromal elements. To mimic the native tissue, chemical, and mechanical properties of the 3D tissue constructs should mimic the characteristics of the native tissues. A gradient of cell types, biomolecules, and other structural and compositional components also needs to be developed in certain types of bioprinted tissue constructs.[59] To address these demands, precise control of shape, flow, and composition of cell-laden fibers during bioprinting is needed. Therefore, methods that allow more precision and control over the organization of materials, cells, and biomolecules in the resulting 3D constructs are needed to accurately mimic the composition of the native tissues.

Recently, microfluidic-based bioprinting technique has been introduced. In this technique, the integration of microfluidic systems with traditional extrusion-based bioprinting facilitates tuning the structural and compositional properties of tissue constructs during the printing. Microfluidic fabrication techniques[60–62] enable the control of minute amounts of liquids,[63–65] cells,[66,67] and molecules.[68,69] It is also possible to empower these systems with various control tools, such as valves[70–72] and sensors.[73–75] It was demonstrated in several studies that microfluidic devices can be used to produce fibers using wet-spinning technique.[76–78] The latter technique can also be used in 3D bioprinting.[79,80] Microfluidic-based 3D bioprinting systems can be used to control cell and molecule deposition, flow, mixing, and gradient building in the resulting 3D structures. Recent studies reported the production of structures, such as fibers,[81–83] hollow structures,[84–86] and various other combinations by using microfluidics-based methods.[87–89] These developments represent an early step toward adding incremental complexities to 3D bioprinted constructs to make biomimetic tissues and organs.

With this in mind, in this paper, previous reports on the development and application of microfluidics in 3D bioprinting are reviewed and current challenges and future directions are presented. In particular, recent advances of extrusion-based 3D bioprinting combined with microfluidic platforms to fabricate tissue constructs are discussed. Finally, obstacles for the translation of such studies to the clinic are described.

2. Extrusion 3D Bioprinting

2.1. Basic Principles

In the last few years, extrusion-based 3D bioprinting has rapidly become one of the most popular approaches in biofabrication.[26,90–92] Current extrusion-based 3D bioprinting strategies can be divided into four different groups: i) direct ink writing (DIW), ii) coaxial printing, iii) coagulation bath printing, and iv) free-form reversible embedding (**Figure 1**). The need to develop different techniques has been driven mostly by limited crosslinking strategies for biomaterials. In general, the crosslinking should be rapid and cell-friendly to guarantee a preserved shape of printed objects and avoid a detrimental collapse of the extruded structure.[93–95]

DIW is one of the first methods that has been developed. This method is based on the extrusion of a highly viscous ink, which show shear-thinning property in many cases.[96–99] In this process, an external force is applied to the cartridge in which the bioink is stored, pushing the bioink to flow through the needle. Upon extrusion, laid hydrogel struts rapidly recover their initial viscosity and stop to flow. This approach has received a huge interest because the shear-thinning property allows an efficient and controllable deposition of bioink. Additionally, one can tune the rheological behavior of bioinks simply by adjusting the concentration of the bioink components [100–102] or formulating complex biopolymer blends.[86,103,104] However, tuning the rheological behavior of a bioink remains a challenge. Bioinks should be formulated to achieve both high printing resolution and cell viability. These features are often hard to achieve. Thus, further attempts are being made to optimize bioink formulations.

In addition to DIW, researchers have developed another extrusion strategy based on the use of coaxial extruders.[82,105–109] This strategy has attracted much attention as it offers several advantages, including high printing resolution and accuracy and the possibility to process several biomaterials and modularity.[110] This printing strategy consists of delivering bioink and a crosslinking solution separately through inner and outer nozzles. In the case of the multiaxial nozzle, the outermost nozzle is used to deliver a crosslinking solution, while the inner nozzles deliver one or more bioinks or templating solutions.[92] In

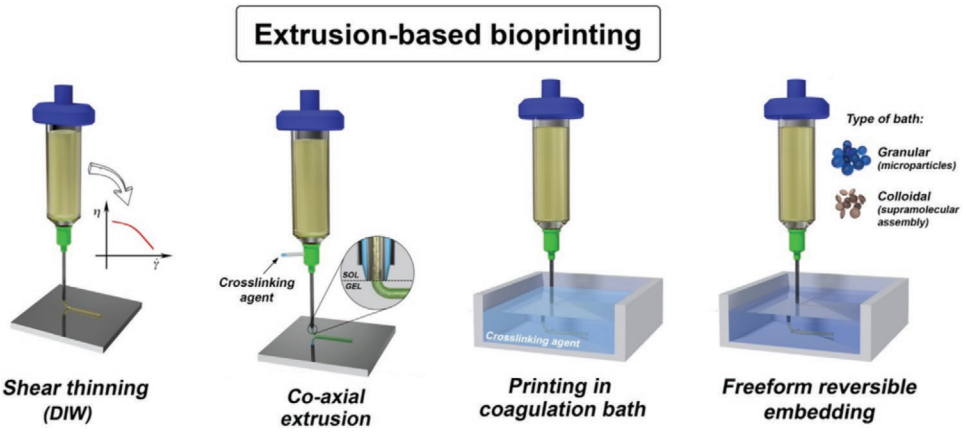

Figure 1. Illustration of the most popular extrusion 3D bioprinting strategies. Reproduced with permission.[92] Copyright 2018, IOP Publishing.

particular, this technique decouples the printing accuracy from bioink rheological behavior.[111,112]

Another approach consists of extruding a bioink directly into a coagulation bath that triggers its gelation.[113,114] Despite the apparent simplicity, this approach has several disadvantages that have limited its use. A major problem is the clogging of bioinks in the nozzle due to the rapid diffusion of the coagulation solution.[92] The lack of proper adhesion between consecutive layers in the 3D construct is another challenge. This often leads to structural instabilities that limit the application of bioprinted materials.[115] Furthermore, it requires rapid bioink gelation. However, this strategy offers high flexibility in material selection.[92]

A more sophisticated approach for extrusion bioprinting involves free-form reversible embedding, which consists of extruding bioink into a pseudoplastic or granular bath.[116–118] In this case, the rheological properties of the bath solution are of great importance. The bath solution generally contains nano- or microparticles that are used as additives to tune the rheological behavior of the bath solution to ensure the bioink stability after extrusion. Such a strategy has been used so far only in a few recent studies[116–118] and continues to attract more attention due to the aforementioned potentials offered in terms of materials selection and tunability. The major drawback of this approach, however, is related to the removal of bath solution from printed structures by which some changes may be applied to the printed geometries.

2.2. Applications

2.2.1. Skeletal Muscle Tissue Engineering

Skeletal muscle contains long multinucleated fibers that are located parallel to each other. As an alternative to the use of autologous muscle tissues to treat volumetric muscle loss, engineering skeletal muscle tissue is required.[119] Engineered constructs need to mimic the function and properties of native tissue. In particular, one should recapitulate the anisotropic, highly aligned architecture of muscle fibers. To this aim, 3D bioprinting technologies seem to be an ideal candidate as they enable us to precisely fabricate such biomimetic structures.[120,121] In addition, engineered muscle tissues can be used as drug screening models.[122] Kim et al. developed a multilayer skeletal muscle construct composed of spatially controlled and aligned myofiber bundles through a method called integrated tissue–organ printing. In their proposed method, human muscle progenitor cells-laden hydrogel as bioink, acellular gelatin hydrogel as a sacrificial layer, and poly(ε-caprolactone) (PCL) polymer as supporting material were bioprinted through extrusion-based technique.[123] The biofabricated skeletal muscle tissue resulted in 82% recovery of tibialis anterior muscle defect compared to normal tissue, eight weeks after the implantation in rats. In another study, Choi et al. developed a decellularized skeletal muscle extracellular matrix (ECM)-based bioink for skeletal muscle fabrication.[50] This bioink could support fabricating 3D structures for skeletal muscle tissue with high cell viability, differentiation, maturation, and contractility. The results revealed uniform distribution of cells with high cell viability (>90%) 24 h after printing showing biocompatibility of the bioink. This bioink could also mimic the native muscle tissue structure and function, which makes it a promising biomaterial for muscle tissue regeneration. To study cell alignment for developing biomimetic skeletal muscle constructs, Mozetic et al. reported the use of direct writing bioprinting method for meticulously print structures made of pluronic/alginate-based hydrogels.[48] Extrusion bioprinting with a pneumatic dispensing syringe was used and the constructs were crosslinked in calcium chloride. Due to shear stress-induced during the bioprinting process, C2C12 murine myoblasts were aligned along the printing direction just after printing and highly elongated 7 days after culture, with cell viability of over 85%. Despite the partial cell alignment achieved and the increased expression of some myogenic genes, after 21 days of culture, a limited number of cells underwent myogenesis with the scarce formation of multinucleated myotubes most likely due to the Pluronic/alginate inert matrix.

2.2.2. Cardiac Tissue Engineering

Cardiac tissue engineering aims to develop 3D tissue constructs that can mimic cardiac tissue structure and function. Cardiac muscle tissue is a striated tissue composed of branched fibers (cardiomyocytes (CMs) with a single nucleus) connected by intercalated disks. The development of a 3D and functional cardiac tissue construct with a native-like tissue matrix, the high population of cells, and rich vascularization that can guarantee a stable and functional contractile tissue is quite challenging.[124] A growing body of research has focused on untangling these challenges by implementing extrusion 3D bioprinting techniques.

3D cardiac tissue constructs can be obtained by using 3D printing of biomaterials combined with appropriate cells. For example, Gaetani et al. bioprinted cardiomyocyte progenitor cells/alginate constructs with various concentrations of sodium alginate (5%, 7.5%, and 10%).[125] The final 3D printed cardiac tissue construct contained a homogenous distribution of the cells. Higher values of alginate content (7.5% and 10%) resulted in the formation of more structurally stable constructs due to higher viscosity of the bioinks. The cell viability of 92% and 89% were obtained after 1 and 7 days of culture, respectively. In another work, Zhu et al. developed a bioink of gelatin methacryloyl (GelMA)-coated gold nanorods (G-GNRs) combined with alginate hydrogels, cardiac fibroblasts, and CMs for bioprinting of 3D cardiac tissues.[108] Introducing GNRs in the bioink not only facilitated the printability due to the shear-thinning effect, but also promoted cell to cell interactions, mitigated overproliferation of cardiac fibroblasts, and led to the synchronized contraction of the tissue. The bioprinting process included coaxial extrusion of the bioink and $CaCl_2$ through internal and external needles of the nozzle followed by UV light exposure for covalent crosslinking of GelMA. Printing speeds of 5 and 10 µL min^{-1} resulted in cell viability of over 70% when the UV light exposure was below 30 s, while higher printing speeds or longer periods of UV light exposure led to decreased cell viability. In another study by Jang et al., stem cell-laden bioinks of heart decellularized ECM (dECM) were developed and used for extrusion-based bioprinting of prevascularized 3D tissues that can mimic the cardiac microenvironment.[126] Multimaterial bioprinting of

prevascularized constructs was enabled by two robotic microextrusion printheads for printing various bioinks laden with different cell types. Alternative printing of cardiac progenitor cell-laden bioink and mesenchymal stem cells (MSCs)-laden bioink patterns were implemented. It was supposed that the patterned prevascularized patch can promote vascularization and enhance cardiac function upon transplantation.

2.2.3. Tubular/Vascularized Tissue Engineering

The cardiovascular system is the first system that develops in embryo and plays an important role in oxygen and nutrient delivery to organs and tissues. Vascularized network in the human body develops through two processes i) vasculogenesis and ii) angiogenesis. Vasculogenesis is the process of de novo blood vessel formation by endothelial cells (ECs), while angiogenesis is the formation of blood vessels from existing vessels.[127,128] Recently, a growing body of literature has emerged around constructing 3D vascularized tissues that try to mimic the native vascularization system. For example, Norotte et al. used micropipettes of 300 and 500 μm diameter to produce smooth muscle cells (SMCs) and fibroblasts containing pellets for extrusion bioprinting of spheroids and cylinders that were used to construct tubular structures in a layer-by-layer fashion.[129] They also used agarose rods as templets (0.9–2.5 mm in diameter). The fusion of bioprinted cellular units occurred and branched tubular structures having multiple layers were obtained (**Figure 2**A).

To engineer a blood vessel-like structure, Skardal et al. used microcapillary (inner diameter of 500 μm) tube-style bioprinting of fibroblast-laden filaments.[130] Tetra polyethylene glycol (PEG) was converted to tetra-acrylate derivatives and used for rapid crosslinking of thiolated hyaluronic acid (HA) and gelatin derivatives (in 10 min). Filaments were printed in a layer-by-layer fashion to form tubular blood vessel-like constructs by using cell-laden filaments and acellular agarose filaments (Figure 2B). After four weeks in culture, there were only a few dead cells. It was thought that using this 3D bioprinting method it can be soon possible to develop functional blood vessels. In a study, hollow fibers were produced and then embedded in multilayer hydrogel to form perfusable constructs, where a pressure-assisted coaxial fabrication system was used.[131] In this study, authors developed cartilage progenitor cell-laden alginate microfluidic channels with an average inner diameter of 135 μm. When the constructs were perfused, there was no blockage or swirling observed (Figure 2C). They suggested that nanofibers can be used to reinforce the channels and improve their mechanical properties. They have also suggested blood vessels can be engineered using triaxial system, SMCs, and ECs. Constructs having perfusable alginate hollow fibers embedded in alginate gel were developed by Zhang et al. using coaxial pressure-assisted robotic system (wall thickness of 200 μm).[132] Hollow fibers were also developed using chitosan but they were found to be fragile. Increasing dispensing rate of the bioink resulted in the formation of enlarged channels and thicker walls, while increasing the crosslinker flow rate resulted in increased channel diameter. Cells were uniformly distributed in the channels. Authors suggested to use SMCs and ECs to engineer blood vessels in future.

Jia et al. provided a 3D bioprinting vascular network by employing an extrusion bioprinting system to print a perusable structure in a highly organized structure.[86] The cell responsive bioink was developed with a combination of GelMA, sodium alginate, and 4-arm PEG-tetra-acrylate (PEGTA). The coaxial extrusion system was used to fabricate the vasculature network. This printing strategy with tunable bioink properties was used to print vasculature structure with different diameter, geometry, and shape. The fabrication mechanism involved two crosslinking processes for the developed bioink. The optimization process revealed that 7% (w/v) GelMA concentration has the best cell responses, 3% (w/v) alginate can improve the printability of bioink and the maximum of 2% (w/v) PEGTA can enhance the mechanical strength of the structure. Human umbilical vein endothelial cell (HUVEC) and MSC cell-laden bioinks were used to produce hollow tubes with an outer diameter of 500–1500 μm, an inner diameter of 400–1000 μm, and thickness of 60–280 μm.

The ability to construct vascular channels on a large scale mimicking the native vasculatures is critical and important for the clinical application of any engineered tissue. To address the survival and proliferation of larger tissues, Lee et al. reported a capillary network and connecting to vascular tissues that can contribute to tissue viability and growth..[47] The microvascular network was formed by EC and fibroblast embedded in fibrin gel between two larger vessels with a size of 0.5–1 mm. In a study by Gao et al., hollow filaments of calcium alginate loaded with fibroblasts were 3D printed layer-by-layer structure using a coaxial nozzle.[133] By tuning the concentration and flow rate of the bioink, crosslinking time, high-strength 3D structures were obtained. The hollow microchannels within the construct improved oxygen and nutrient supply to cells residing in the construct, and thus cell viability was improved. In this study, cell viability was 67 ± 4% after 7 days when utilizing the 3D alginate scaffolds with hollow fibers, which is higher than that observed using solid fibers (50 ± 1.6%) after 7 days.

2.2.4. Osseous and Chondral Tissue Engineering

Bone is a highly vascularized tissue. Cortical bone is formed of parallel cylindrical units or osteons where each osteon includes a central canal surrounded by concentric rings (lamellae). Bone cells in osteons (osteocytes) exist in free spaces between these rings called lacunae. Bone connects to the cartilage at joint ends. Cartilage is a tough connective tissue that is more flexible compared to the bone. Articular hyaline cartilage lacks blood vessels, lymphatics, and nerves. The native cartilage is transited to the bone in a gradient way.[134] Shim et al. employed a multihead bioprinting system for constructing 3D porous osteochondral tissue.[135] The integrity of the 3D tissue was maintained through printing a framework of PCL surrounding the construct. The PCL was dispensed in the form of a porous framework and two bioinks of alginate loaded with osteoblasts and chondrocytes were sequentially bioprinted in the pores. Osteoblasts and chondrocytes showed the viability of 95% and 93%, respectively, after 7 days post-printing. In another study, Kesti et al. developed a chondrocytes-laden bioink consisted of gellan, and alginate integrated with the cartilage ECM particles.[136]

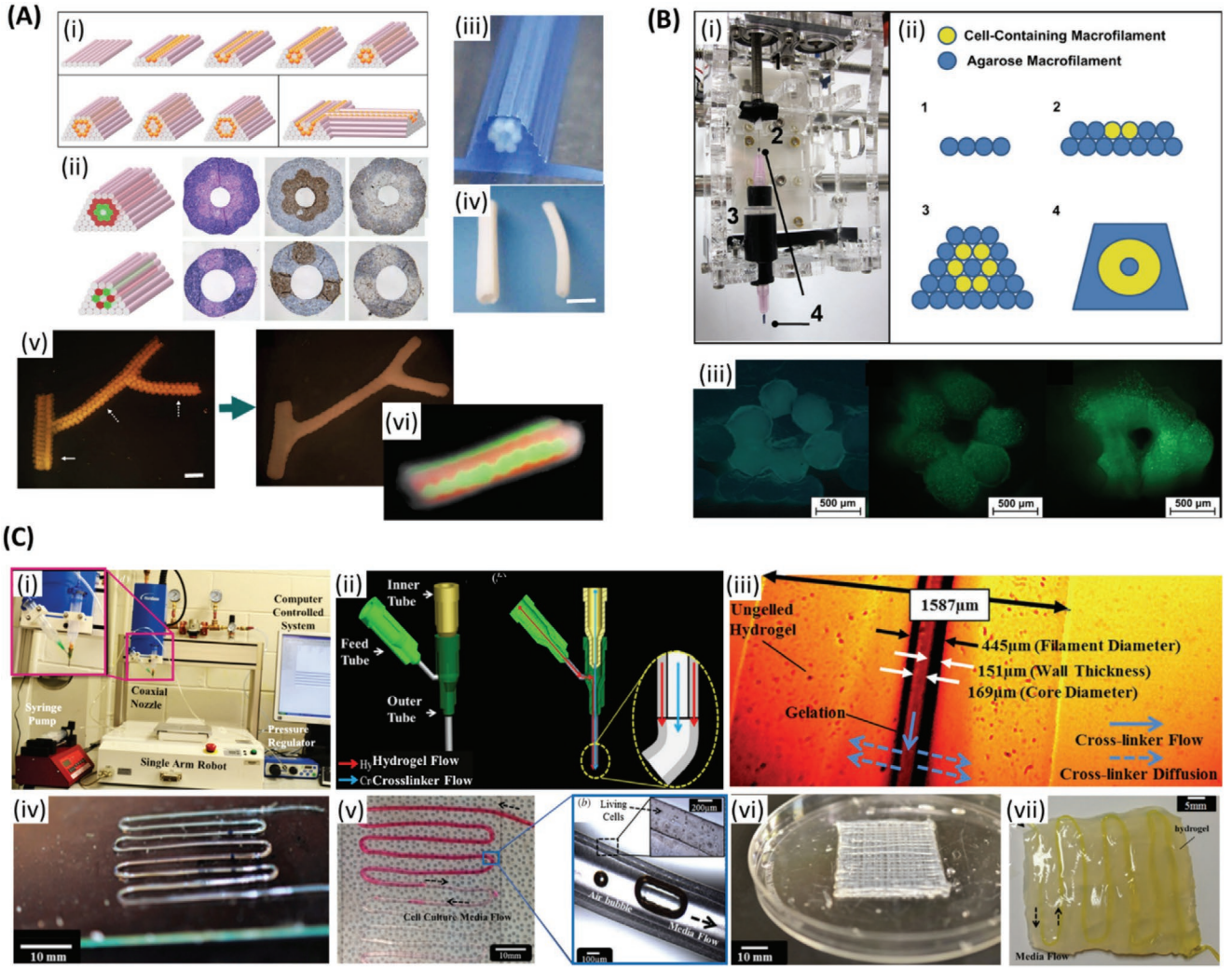

Figure 2. Extrusion bioprinting of vascularized tissue. A-i) Complex 3D tubular structures formation through layer-by-layer deposition of agarose rods (pink) and multicellular spheroids (orange). ii) Tubular structures based on two different patterns with multicellular double-layer wall (green: human umbilical vein smooth muscle cells (HUVSMCs); red: human skin fibroblasts (HSFs)) before and after 3 days of fusion. iii) Printed tubular construct. iv) Bioprinted pig smooth muscle cells (SMCs) tubes with different diameters after 3 days of fusion. Outer diameters are 2.5 mm (left) and 1.5 mm (right). v) Printed branched structure just after printing (left) and the final fused structure after 6 days (right). Spheroids are 300 µm and branches pointed with solid and broken arrows are 1.2 and 0.9 mm, respectively. vi) Fluorescent image of the tubular structure showing the fusion pattern after 7 days of printing. Scale bars: iv) 2.5 mm and v) 1.2 mm. Reproduced with permission.[129] Copyright 2009, Elsevier. B-i) A customized adaptor for microcapillary-based printing. ii) Developing a tubular structure through layer-by-layer printing of cell-encapsulated hydrogel microfilaments. iii) Fluorescent images of the cross-section of cell-laden tubular constructs just after printing, after 14 days and 28 days of culture, respectively. (green: live cells; red: dead cells). Scale bars: 500 µm. Reproduced with permission.[130] Copyright 2010, Elsevier. C-i) Single-arm robotic printer with coaxial nozzle. ii) Schematic of the coaxial nozzle with hydrogel and the crosslinker flow. iii) The influence of the hydrogel properties in the dimensions of the hollow filaments. iv) A single-layer microfluidic channel network. v) Media flow through bovine cartilage progenitor cell-laden alginate microchannel. vi) An eight-layer microfluidic channel network. vii) Microfluidic channel embedded in bulk hydrogel. Scale bars: iv) 10 mm, v) 10 mm, magnified image: 100 µm, vi) 10 mm, and vii) 5 mm. Reproduced with permission.[131] Copyright 2013, IOP Publishing.

The bioink was extruded sequentially with the help of polymeric support to maintain the structural integrity of the overhanging regions. The proposed printing process included: 1) Loading the bioink and polymeric support (mixed with small amounts of cations) in separate syringes and extruding sequentially. 2) Diffusion of the cations from the support material to the periphery of printed construct where crosslinking is initiated. 3) Cell-friendly crosslinking of the final construct through immersion in a 4 °C medium (containing cations) along with removal of the support. An adult nose-shape construct was bioprinted with this method, and it showed a cell viability of 96% in the periphery and 60% in the center of the construct 7 days after bioprinting.

2.2.5. Skin

Skin, as the largest organ in the human body, serves as a physiological barrier that protects the internal organs from the external physical and chemical threats. It consists of three

main layers, including the epidermis, dermis, and hypodermis that contain nerve and blood vessels. The epidermis consists of keratinocytes that form a stratified epidermal cell layer which plays an important role in protection by acting as a physical barrier. The dermis consists of two layers of interconnected collagen and elastin fibers along with dermal fibroblasts. The last and deepest layer of skin, the hypodermis, is made of vascularized adipose tissue. 3D bioprinting technologies hold promising potential for creating skin tissues due to the highly organized, layer by layer structure of human skin. Shi et al. developed a collagen and GelMA-based bioink with two steps crosslinking for extrusion bioprinting of skin scaffolds. The bioink (GelMA 5% w/v and collagen 8% w/v with various ratios of tyrosinase) was mixed with human melanocyte cell line (HEM), human keratinocyte cell line (HaCat), and human dermal fibroblast cell line (HDF). A 200 μm nozzle and the pressure of 0.8–1.2 bar were used during bioprinting. This study demonstrated that tyrosinase can increase HEM proliferation while inhibiting HDF growth. Moreover, tyrosinase showed no significant effect on the growth and activity of HaCat cells.[137] Admane et al. produced a human skin model with similar thickness to the human skin by an extrusion-based bioprinter to understand cell signaling pathways for drug screening applications. This work fabricated a dual-layered skin of epidermal and dermis layers. A 5% w/v silk fibroin and 5% gelatin bioink were used to print a 14 layered dermal structure with the optimized parameters and the epidermal layer was printed after day 3 to mimic the structure of human skin. The printed scaffold demonstrated the biochemical and mechanical properties of human tissue. In addition, keratinocytes in the epidermis layer construct showed migration of these cells between scaffold pores. Proteomic and transcriptomic analysis in this study revealed the similarity between signaling pathways in 3D printed skin models and human skin.[138] Finally, Jorgensen et al. demonstrated a trilayer bioprinted skin model composed of human keratinocytes, melanocytes, fibroblasts, dermal microvascular endothelial cells, follicle dermal papilla cells, and adipocytes using a fibrinogen bioink to mimicking human skin. The bioprinted model was evaluated in terms of forming the epidermal barrier and collagen remodeling to be used as a graft for wounds. The results of this study showed an increase in wound closure by epithelization and advancing epidermal barrier integration followed by collagen remodeling. The proposed methods in human skin bioprinting could be utilized for treatment of full thickness wounds to recapitulate human skin. [139]

2.3. Limitations

Extrusion 3D bioprinting techniques are powerful tools for the engineering of constructs that can closely resemble the native tissues.[10,28,140] However, these methods suffer from some disadvantages and they pose challenges. The first and major drawback is the limited number of biomaterials available for bioink formulation.[13,95] Therefore, in order to improve the performance of 3D bioprinted constructs and printing capacity, researchers have to: i) formulate new blends out of available biopolymers,[141–143] ii) include additives (e.g., particles and fibers) in the bioink formulation or introduce new groups via chemical modification,[94,144,145] and iii) develop new 3D bioprinting and crosslinking methods. However, improving the printability of ink generally implicates a decrease in cell viability and matrix suitability for cell proliferation, spreading, and maturation. Another common issue is related to the limited degree of biomimicry of currently developed bioinks. These bioinks often contain synthetic (e.g., Pluronics[146–148]) or natural polymers (e.g., alginate[149–151] and chitosan[152–154]) that are not found in the native ECM and thus bioprinted constructs are not capable of remodeling. The ECM plays a key role in tissue regeneration by directly modulating cellular response and behavior.[155–157] Thus, bioinks should also be formulated to mimic the native ECM to prompt rapid and efficient feedback from the contained cells. Toward this direction, some studies have used dECM as bioinks.[50,158,159] However, additional work is required to improve dECM mechanical properties and stability as it tends to rapidly degrade during culture.[160] Another important issue that still has to be addressed is how to enable the simultaneous deposition of multiple cells and biomaterials to fabricate complex and heterogeneous structures.[161] This feature is essential to mimic the structural organization of the native tissues and to recapitulate their functionalities in vitro. In the past few years, an increasing number of studies have partially addressed this topic.[105,162–164] However, printing resolution (≈0.1–1 mm)[13,165] and structural complexity of the printed structures are not quite satisfactory and a great deal of work is still needed.

New printing techniques should be developed to increase the accuracy of cell and material deposition. Moreover, the typical printing speed of extrusion bioprinting systems is in the range of 10–50 μm s^{-1}, which is lower than that of other 3D bioprinting systems, such as drop-on-demand bioprinting (1–10 000 droplet s^{-1})) and laser bioprinting (200–1600 mm s^{-1}).[166] The bioprinting speed is a key important parameter for future scale-up of technologies and obtaining engineered constructs in clinically relevant sizes.[115] Finally, the high volume of bioprinted constructs will require addressing a well-known tissue engineering problem, the integration of a functional vasculature within the bioprinted constructs.[115,167] Despite a number of studies have addressed this challenge,[168–170] a reliable strategy is still lacking, especially for the manufacturing of microvascularized system.[167]

2.4. Recent Advances: Integration of Microfluidic Techniques

Extrusion 3D bioprinting technique remains as one of the most popular strategies in 3D biofabrication[171] and researchers are constantly improving this method. One of the main recent advances in the field is the integration of microfluidic systems to extrusion 3D bioprinters. [79,80] Such devices represent a breakthrough, as they enable: i) a precise manipulation of volume of bioinks to be extruded,[161] ii) simultaneous extrusion of multiple inks through the same nozzle (thus allowing to fabricate heterogeneous structures that can better mimic the native ECM and cellular organization),[115,161] and iii) possibility to create a priori complex bioink patterns,[105,111] graded [172] or layered structures[85,109] that can be precisely laid down as fibers thanks to low Reynolds number that prevents bioink mixing.

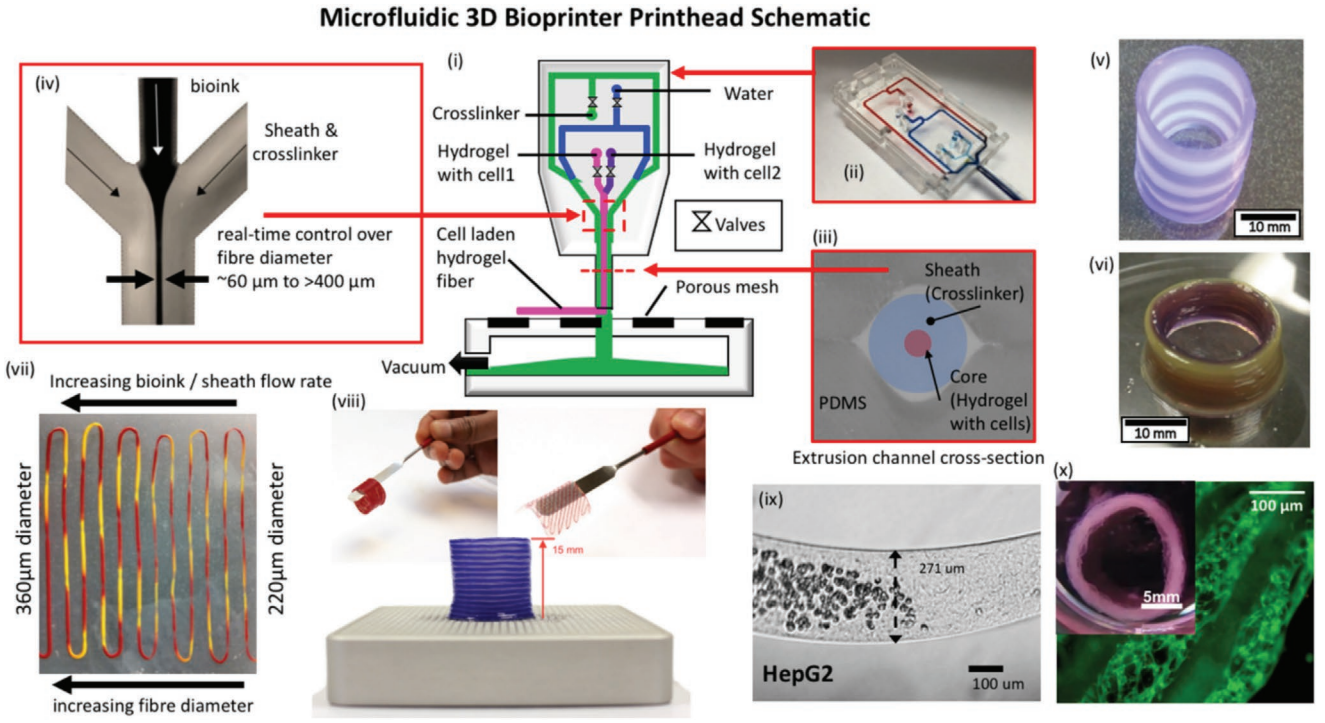

Figure 3. Microfluidic bioprinting principles. i) Schematic of a microfluidic 3D bioprinting system depicting a ii) two material PDMS microfluidic printhead with integrated pneumatic valves and iii,iv) coaxial flow focusing extruder capable of generating hydrogel fibers with diameters ≈60 to > 400 µm. Integration with a 3-axis positioning system and custom software enables a variety of multimaterial structures to be fabricated including. Reproduced with permission.[79] Copyright 2013, IEEE. v) Tubular structures with inter-layer switching and vi) concentric tubular structures with in-plane intralayer material switching. Flow control over the ratio of hydrogel and crosslinker flow rate enables vii) sequenced 2-material fibers with on-the-fly control over fiber diameter. viii) Printed alginate structures are robust and can be manual manipulated directly postprinting. ix) Abrupt switching between regions containing cells and those without cells is possible. A variety of different cells have been validated in the hydrogel fiber platform including x) human airway primary smooth muscle cells in an alginate collagen fiber and cultured to produce a functional airway contraction model.

All these advantages have brought new potentials for enabling the fabrication of advanced constructs. The complexity of bioprinted structures have been greatly increased when compared with conventional extrusion bioprinting systems, and thorough studies are required to exploit the full potential of these systems. However, in order to transfer the results from laboratory to clinic,[173] such advances should be accompanied by an improvement of bioink formulation and reduction of printing time.

3. Microfluidic Bioprinting

3.1. Basic Principles

Microfluidic devices allow bioprinting with highly precise control over small amounts (10^{-9} to 10^{-18} L) of fluids through designed channels that are in the scale of tens of micrometers in diameter. This enables a supreme control over fluid in space and time. Microfluidic chips include mainly channels and fluid reservoirs, which reduce manufacturing cost, disposal, chemical reagent consumption, and analysis time. Microfluidic chips have found many applications, such as molecular analysis, separation, diagnosis, as well as drug discovery and development. Their control overflow and capability of mixing cells with bioinks in a controllable manner make the use of microfluidic systems an attractive tool to integrate into 3D bioprinting technology. [174–176]

In microfluidics-assisted 3D bioprinting, fluid bioink flows through microchannels (**Figures 3** and **4**A,B), which allows control of flow,[79,80,177] switching,[80] and mixing of components,[18,178] in a precisely controlled manner.[179,180] Moreover, microfluidic bioprinting is associated with reduced shear stress during the process. This can be attributed to the sheath flow surrounding the laminar core.[181] In addition, efficient control of morphology,[181] dimensions,[182] and direction of produced objects can be achieved. When combined with extrusion bioprinting, microfluidic processing can improve the resulting resolution of the printing procedure[112] beyond the current resolution of microextrusion (≈50 µm).[91]

3.2. Technique

Bioink, the basic cell-laden biomaterial used when 3D bioprinting, is prepared in a fluidic form and then fed into printer either in one mixture or separate portions with a cross-linker that are mixed in the printing device or at its nozzle. Moreover, a multinozzle system can also be used in microfluidic bioprinting. Bioinks may also be extruded separately, and then combined after they exit from independent orifices, to produce structures having core–shell composition.[183] Although different approaches of microfluidic bioprinting were developed by different groups,[18,80,189,112,129,181,184–188] further improvements

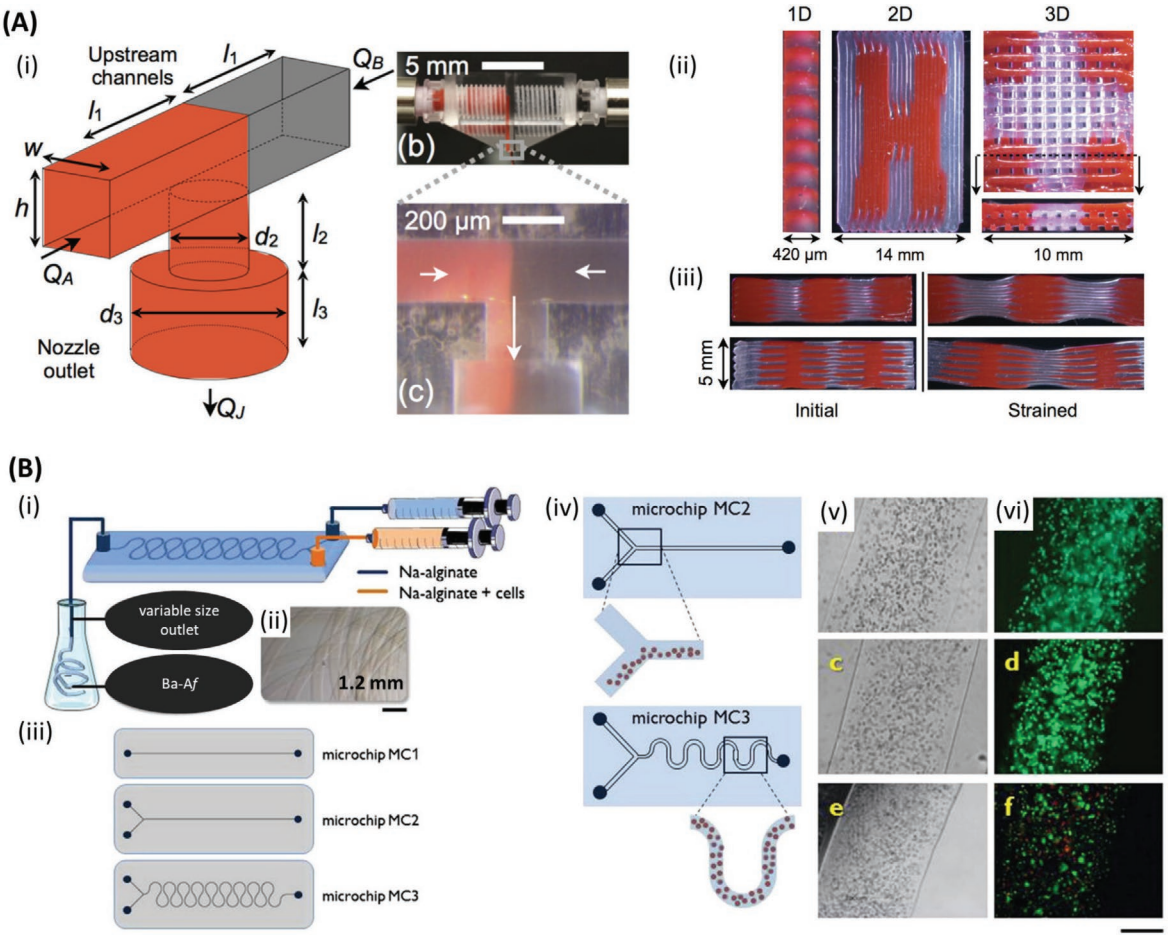

Figure 4. Microfluidic bioprinting chips. A-i) Schematic of a microfluidic printhead for multimaterial printing with controlled flow rate of each material by independently actuated syringe pumps. ii) 1D, 2D, and 3D printed multimaterial PDMS (red and clear) structures. iii) Cross-section images of two different multimaterial 3D structures with different stiffness. Initial form of the structures (left), and after applying strain (right). Reproduced with permission.[184] Copyright 2015, Wiley-VCH. B-i) Schematic of the microfluidic chip for alginate microfibers formation. ii) Micrograph image of the alginate microfiber formed by microfluidic chip. iii) One and two inlets straight channel microfluidic chips (top and middle) and two inlets snake-shape channel micromixing chip (bottom) for cell-laden alginate microfibers formation. iv) Schematic of segregated versus homogenous cell distribution within alginate microfibers when employing straight channel and snake-shape channel microchips. v) Optical and vi) fluorescent images of sarcoma osteogenic (SaOS-2) osteoblast-like cells laden in alginate microfibers after 1 day (top (both)), 7 days (middle (both)), and 14 days (bottom (both)). (green: live; red: dead). Scale bar: 250 µm. Reproduced with permission.[181] Copyright 2015, Elsevier.

in the efficiency of bioprinting processes are still needed. In microfluidic printing, a T or Y chip can be used for feeding multimaterials into the printing head (Figure 4A).[184] Two opposed syringe pumps can be alternately used for pushing inks through two channels into a single nozzle, to print constructs having a sharp transition between different constituent materials. **Table 1** summarizes various designs of the microfluidic channel and needle-based production of microfibrous structures. Beyer et al. demonstrated the first complete 3-axis multimaterial 3D bioprinting system utilizing coaxial flow-focusing with integrated valves in disposable polydimethylsiloxane (PDMS) printheads and crosslinker removal (Figure 3).[79,80] The use of integrated microfluidics enables on-the-fly switching between cell/hydrogel sources and control over flow rates in the crosslinker. Multiple channels enable on-the-fly modulation of fiber diameter and abrupt switching between cell-laden and cell-free regions. Custom slicing algorithms enable interlayer and intra-layer material switching and creation of complex patterns within layers and across 3D constructs. Angelozzi et al. found that the use of two-inlet, snake-like micromixing chip is more efficient in bioprinting homogenous distribution of cells within osteoblast-laden alginate microfibers.[181] Alternatively, the use of straight channels was found to lead to the segregation of cells along one side of resulting fibers due to the dispersion of particulate matter occurring in the laminar flow of microfluidic devices (Figure 4B). In one study, Nie et al. demonstrated the use of capillary coaxial microfluidic bioprinter for the production of porous 3D structures.[81] In the latter work, alginate hydrogel was loaded in the printer and crosslinking solution ($CaCl_2$) was employed in the sheath fluid. At first, the vacuum was set to a high level, and the 5–6 bottom layers were printed as sacrificial layers for a better resolution printing of the final construct on top of that, with the vacuum set to its low level. This technique offers 10 times faster printing compared to systems, which are capable of 3D printing at the same resolution. The coaxial system is useful for processing polymers

Table 1. Reports on the use of microfluidics in bioprinting (P) and in producing cell-laden microfibers (F) using microchannel-based (C) or needle-based (N) systems. Studies showing cell types, biomaterials, and fabrication methods.

Study	Cells	Biomaterial	Method	P/F	C/N	Tissue	Ref.
Production of cell-loaded microfibers	Bovine carotid artery vascular endothelial cells (ECs)	Alginate	Needle extrusion of alginate in coflowing stream of $CaCl_2$	F	N	Not specific	[285]
A novel microfluidic-based technique for continuous formation of microfibers	Human fibroblasts; bovine serum albumin (model for biomolecules)	Alginate	Microfluidic coaxial flow of alginate in the core and $CaCl_2$ in the sheath	F	C	Not specific	[286]
Formation of cell-laden tubular hydrogels in laminar flow stream	Human kidney 293 cells	Alginate	Microfabricated silicon nozzle array is used to simultaneously produce multiple microfibers by extruding alginate solution into a stream of $CaCl_2$ solution	F	N/A (micronozzle (MN) array)	Not specific	[287]
Fabrication of 3D architected tissue constructs to be utilized as pharmacokinetic models	Hepatocytes HepG2	Alginate	Syringe-based direct cell writing (DCW) is used to fabricate 3D micro-organ and is followed by soft lithographic micropatterning to create in vitro device	P	N	Not specific	[288]
Fabrication of cell-laden alginate hollow fibers	Human iliac vein endothelial cells (HIVE-78); bovine serum albumin (model for biomolecules)	Alginate	Microfluidic chip and coaxial flow	F	C	Not specific	[289]
Formation of alginate microfibers	*E. coli*; yeast	Alginate, carboxylate polymer beads and silver nanoparticles	Roller-assisted microfluidic system (forming by microfluidic chip into a $CaCl_2$ bath)	F	C	Not specific	[182]
Fabrication of scaffold-free vascular tubular grafts	Various vascular cell types, including smooth muscle cells (SMCs) and fibroblasts	Agarose rods and multicellular spheroids	Computer-aided bioprinting with separate printheads for extrusion of agarose rods and multicellular cylinders	P	N/A (micropipette)	Not specific	[129]
Vessel-like cell-laden constructs	NIH 3T3 fibroblasts	Cell-laden TetraPAc-crosslinked synthetic extracellular matrices (sECMs), polyethylene glycol diacrylate (PEGDA)-crosslinked sECMs, and acellular agarose macrofilaments	Microcapillary tube extrusion system	P	N/A (microcapillary tube)	blood vessel	[130]
Cell-laden microfibers	Human hepatocellular carcinoma (HepG2)	Alginate or alginate-chitosan	Coaxial flow microfluidic chip	F	C	Not specific	[77]
Cell-laden microfibers	Wharton's Jelly mesenchymal stem cells (MSCs); human myeloid leukemia K562 cells	Alginate	Forming by microfluidic chip into a $BaCl_2$ bath	F	C	Not specific	[290]
Microfluidic fabrication of cell-laden continuous fibers	Hepatocytes; fibroblasts; embryonic neural cells (on surface); neutrophil culture	Alginate	Microfluidic system with several independently controllable inlets	F	C	Not specific	[291]
Microfluidic fabrication of hydrogel microfibers for guided cell growth and networking	Fibroblasts (3T3); human cervical cancer cell line (HeLa); rat pheochromocytoma cell line (PC12)	Cell laden soft core (alginate) sandwiched between solid layers of propylene glycol alginate (PGAL), surrounded by poly-L-lysine (PLL) membrane	PDMS microchannel with separate inlets for sodium alginate solutions with cells in core and without cells in shell	F	C	Not specific	[233]

Table 1. Continued.

Study	Cells	Biomaterial	Method	P/F	C/N	Tissue	Ref.
Microfibers loaded with hepatocytes at center sandwiched by 3T3 cells	Hepatocytes; 3T3 fibroblasts	Alginate	PDMS microchannel with separate inlets for suspensions of sodium alginate with 3T3 cells and hepatocytes	F	C	Liver tissues	[188]
3D alginate constructs	N/A	Alginate	3D printing by coaxial flow focusing microfluidic printhead	P	C	Not specific	[79]
Developing a microfluidic-based 3D bioprinter with on-the-fly multimaterial switching capability	N/A	Alginate	3D printing by coaxial flow focusing microfluidic printhead	P	C	Not specific	[80]
Microfluidic production of long cell-laden core–shell fibers	Fibroblasts (NIH/3T3); myocytes (C2C12, CM (rat primary)); endothelial cells (HUVEC (human primary), MS1); nerve cells (cortical cells (rat primary), neural stem cells (mouse primary)); epithelial cells (HepG2, MIN6m9, HeLa)	Shell is alginate. Core is either pepsin-solubilized type-I collagen (PCol), or acid-solubilized type-I collagen (ACol), or fibrin	formation of a core–shell fiber using double-coaxial laminar flow microfluidic device	F	N	Various	[190]
Fabrication of tubular channels resembling natural vessels	Bovine cartilage progenitor cells	Alginate	New coaxial system by pressure-assisted robotic bioprinting	P	N	Blood vessel	[292]
Developing bioprinting system for cell-laden hollow fibers	Bovine cartilage progenitor cells	Alginate	Manufacturing tubular microchannels by a pressure-assisted robotic system with coaxial nozzle	P	N	Not specific	[131]
Production of cell-laden vessel-like fibers and vascular network	Bovine cartilage progenitor cells	Alginate and chitosan	Coaxial bioprinting of microfibers and embedding in bulk hydrogel	P	N	Not specific	[132]
Developing a multiarm bioprinter for hybrid formation of cell-laden 3D constructs	Cartilage progenitor cells	Alginate	Coaxial system (alginate core and $CaCl_2$ sheath)	P	N	Not specific	[185]
Fabrication of reinforced vascular conduits	Human coronary artery smooth muscle cells	Alginate reinforced with carbon nanotubes (CNTs)	Coaxial bioprinting (sodium alginate as sheath and crosslinker in the core)	P	N	Not specific	[293]
Development of cell-encapsulated 3D hydrogel constructs	Human embryonic kidney (HEK-293) cells	Alginate	Coaxial bioprinting integrated with declogging mechanism	P	N/A (glass capillaries)	Not specific	[83]
ECM-alginate microfibers produced by microfluidics	sarcoma osteogenic osteoblast-like cells (SaOS-2)	Alginate with gelatin or particulate ECM	Microfluidic chip with the outlet tube immersed in a gelling solution	F	C	Bone	[181]
Development of 3D constructs of cell-laden alginate microfibers	Fibroblasts (NIH/3T3 cells)	Alginate	Microfluidic chip for printing on a magnetic substrate (magnet-driven assembly)	P	C	Not specific	[294]
Development of 3D constructs of hollow cell-laden calcium alginate microfibers	L929 mouse fibroblasts	Calcium alginate	Coaxial bioprinting with motorized Z stage	P	N	Not specific	[133]
Developing a novel microfluidic dispenser for integrating with inkjet bioprinters (Lab-on-a-Printer technology)	N/A	Alginate and collagen	PDMS microfluidic passive mixer directly integrated with PDMS/SU8 inkjet dispenser	P	C	Liver	[18]
Fabrication of branched hollow fibers	Mouse fibroblasts	Alginate	Triaxial extrusion	P	N	Blood vessel	[295]

Table 1. Continued.

Study	Cells	Biomaterial	Method	P/F	C/N	Tissue	Ref.
Developing a novel 3D printing system with redesigned printhead for fabrication of 3D vascularized tissue	*E. coli*; human umbilical vein endothelial cells (HUVECs)	Alginate	Coaxial extrusion; $CaCl_2$ (inner needle) surrounded by alginate (extruded into $CaCl_2$ bath)	P	N&C	Blood vessel	[187]
High-resolution bioprinting of cell-laden 3D constructs using low viscose cell-encapsulated alginate as bioink	Human umbilical vein endothelial cells (HUVECs); primary rat cardiomyocytes (CMs)	Alginate and gelatin methacryloyl (GelMA)	Coaxial extrusion; alginate-GelMA bioink through internal needle and $CaCl_2$ through external needle followed by two-step crosslinking	P	N&C	3D cardiac tissue, etc.	[111]
Bioprinting 3D endothelialized scaffolds for manufacturing aligned myocardium	Human umbilical vein endothelial cells (HUVECs); primary rat neonatal cardiomyocytes (CMs); human induced pluripotent stem cells (hiPSCs)	Mixture of alginate, gelatin methacryloyl (GelMA), and photoinitiator (Irgacure 2959)	Coaxial bioprinting of endothelialized scaffolds, seeding with cardiomyocytes and housing in the designed perfusion bioreactor	P	N	Endothelialized myocardium	[107]
Bioprinting of perfusable vessel-like tubular constructs	Human umbilical vein endothelial cells (HUVECs); human mesenchymal stem cells (hMSCs)	Blend bioink of gelatin methacryloyl (GelMA), alginate and polyethylene glycol-tetra-acrylate (PEGTA)	Single step multilayered coaxial extrusion	P	N	Not specific	[86]
Development of porous 3D constructs made from calcium alginate microfibers	N/A	Calcium alginate	Capillary coaxial microfluidic bioprinting on a vacuum substrate	P	N	Not specific	[81]
Development of 3D constructs made from unidirectionally aligned cell-laden hydrogel fibers	Muscle cell precursors (C2C12); fibroblasts (BALB/3T3)	Alginate and semisynthetic biopolymer (PEG-fibrinogen)	Custom-built bioprinter with coaxial extrusion system and programmable microfluidic pumps	P	N	muscle tissue	[106]
Developing modular bioinks of single cell microgels blended with prepolymers for microextrusion bioprinting of 3D constructs	Mesenchymal stem cells (MSCs); bovine chondrocytes; endothelial cells (ECs)	Polyethylene glycol diacrylate (PEGDA) for microgels, then blended with various materials	Microfluidic flow focusing device to emulsify cell-laden prehydrogel in oil phase and produce single-cell-laden microgels which were then incorporated into various materials to produce macroconstructs using various fabrication methods	P	N&C	Not specific	[186]
Development of continues cell-laden hydrogel microfibers in various shapes (solid and hollow) and also 3D constructs by automated assembly	Human umbilical vein endothelial cells (HUVECs); MG63 cells	RGD (Arg-Gly-Asp)-modified alginate	Continues extrusion in various shapes by microfluidic chip	P	C	Not specific	[210]
Development of vascularized 3D cell-laden constructs	Human umbilical vein endothelial cells (HUVECs)	Gelatin methacryloyl (GelMA) blended with alginate	Coaxial bioprinting followed by photocrosslinking,	P	N	Not specific	[197]
Development of 3D multicellular vascular constructs with multilevel fluidic channels	Mouse fibroblasts (L929); mouse smooth muscle cells (MOVAS); human umbilical vein endothelial cells (HUVECs)	Alginate	Coaxial bioprinting of hydrogels encapsulated with different cell types through two separate coaxial nozzles	P	N	Functional vessels	[88]
Development of 3D cell-laden constructs with tuneable microenvironment	Various cells (HUVECs, MDA-MB-231, MCF7 breast cancer cells, and NIH/3T3 mouse fibroblasts)	Cell-laden gelatin methacryloyl (GelMA) in the core and alginate as sheath	Coaxial bioprinting of core/sheath microfibers followed by photocrosslinking	P	N	Not specific	[296]
Development of full-thickness chondral scaffolds with cell and material gradients	Human mesenchymal stem cells (hMSCs) and human articular chondrocytes (hACs)	Gelatin methacryloyl (GelMA), methacrylated hyaluronic acid (HAMA), chondroitin sulfate (CS)- 2-aminoethyl methacrylate (AEMA) and alginate	Microfluidic bioprinting coupled with coaxial extrusion	P	N&C	Cartilage tissue	[172]

that have slow gelation, such as the ECM proteins, and hence they cannot be printed directly in one phase by microfluidic bioprinting.[190] In such cases, a coaxial processing method can be used to develop core–shell fibers that can maintain fiber integrity by forming a shell formed by faster gelling calcium alginate.[191] This allows sufficient time for the ECM proteins, such as collagen and fibrin to become a gel. Afterward, alginate can be selectively removed by using alginate lyase. Gelation of core pregel can be achieved by incubation at 37 °C for collagen and treatment with thrombin for fibrin inside the calcium alginate shell. Using the core–shell method, microfibers loaded with various types of cells including fibroblasts, myocytes, ECs, nerve cells, and epithelial cells (in the core) could also maintain their shape after shell removal. It was also observed that the initial ECM proteins were gradually replaced by newly cell-laden ones.[190] **Table 2** summarizes various types of cells used in microfluidic bioprinting. Not only the cells, but also particulate elements may be included in bioprinted fibers, such as carboxylate, silver nanoparticles,[182] or particulate ECM.[181] Furthermore, a gradient of cells, biomolecules, and biomaterials can also be built using microfluidic bioprinting.[192]

Using microfluidic systems, not only cell-laden microfibers but also few[193] to one cell encapsulation,[186,194,195] or microniches[194] can be produced (**Figure 5**A,B). Microgel encapsulation was found to prolong the residence of injected cells and soluble factors in vivo.[195] Using this strategy, tissues can be built up block by block, in a controlled fashion.[186,194,195] By emulsifying an MSC and chondrocyte containing photocrosslinked poly(ethylene glycol) diacrylate (PEGDA) prehydrogel in an oil phase using a microfluidic flow-focusing device and then crosslinking, droplets containing coated single cells were produced and subsequently used for microextrusion (Figure 5C).[186] Fast on-chip stabilization was used for preventing droplet coalescence. Moreover, cell viability was more than 70%. Microgels were incorporated into other biomaterials to produce macroconstructs. For example, they were incorporated into alginate/GelMA mixtures by using 3D printing. Uniform distribution of microgels was observed. In one study, MSCs and ECs were encapsulated into a proangiogenic fibrinogen material and subsequently cultured for one week.[186] This resulted in the formation a vascularized construct. Although, microfluidic 3D bioprinting can be used to produce objects of

Table 2. Reported types and forms of the cells used in microfluidic bioprinting (MF). Studies showing the bioprinting method, material, cell viability, structure, and long-term durability (time).

Method	Material	Cell	Form	Viability	Structure	Time	Ref.
Micropipette, extrusion	Agarose	Smooth muscle cells (SMCs); fibroblasts	Spheroids	N/A	vessel like	N/A	[129]
MF	Pluronic F-68	Human monocytic U937 cells	Single cell	over 80% for up to 4 days	Single mammalian cells	4 days	[232]
MF	Agarose	R1 and YC5–YFP–NEO murine embryonic stem cells (ESCs)	Microbeads (microgels)	79.6 + 2.5% and 80.0 + 1.6% (for R1 and YC5–YFP–NEO mES cells, respectively) at immediately after transfer to the buffer	Microbeads (microgels)	N/A	[297]
MF	Alginate	Hepatocytes; fibroblasts	Microorganoids	≈80% over 30 days	Cord-like microorganoid	90 days	[188]
MF	Fibrinogen in hyaluronic acid (HA)	Human mesenchymal stem cells (hMSCs)	Single cell microbeads	70% after 24 h	Microniches	4 weeks	[298]
Concurrent printing (extrusion + spheroid deposition)	Alginate	Cartilage progenitor cells (CPCs)	Spheroids and filament	43.92 ± 0.04% for filaments and 60.15 ± 0.05% for spheroids at day 1; 76.06 ± 0.04% for filaments and 79.99 ± 0.06% for spheroids at day 4; 87.23 ± 0.03% for filaments and 92.87 ± 0.02% for spheroids at day 7	3D structure of filaments with cell spheroids deposited in between	2 weeks	[185]
MF	Gelatin methacryloyl (GelMA)	Bone marrow derived mesenchymal stem cells (BMSCs)	Microspheres	>60% for 7 days	Microspheres	Cell differentiation was studied for 28 days	[299]
MF	Polyethylene glycol diacrylate (PEGDA)	L929 mouse fibroblast cells; human embryonic kidney cells (HEK-293); breast cancer cells (MCF-7)	Microstructures	Higher than 80% after 3 days	Different micro-structure shapes	3 days	[300]
MF + microextrusion	Fibrinogen, gelatin methacryloyl (GelMA), polyethylene glycol diacrylate (PEGDA	Multipotent human mesenchymal stem cells (MSCs); bovine chondrocytes; endothelial cells	Single cells (microgels)	More than 70%	3D modular constructs	1 week	[186]

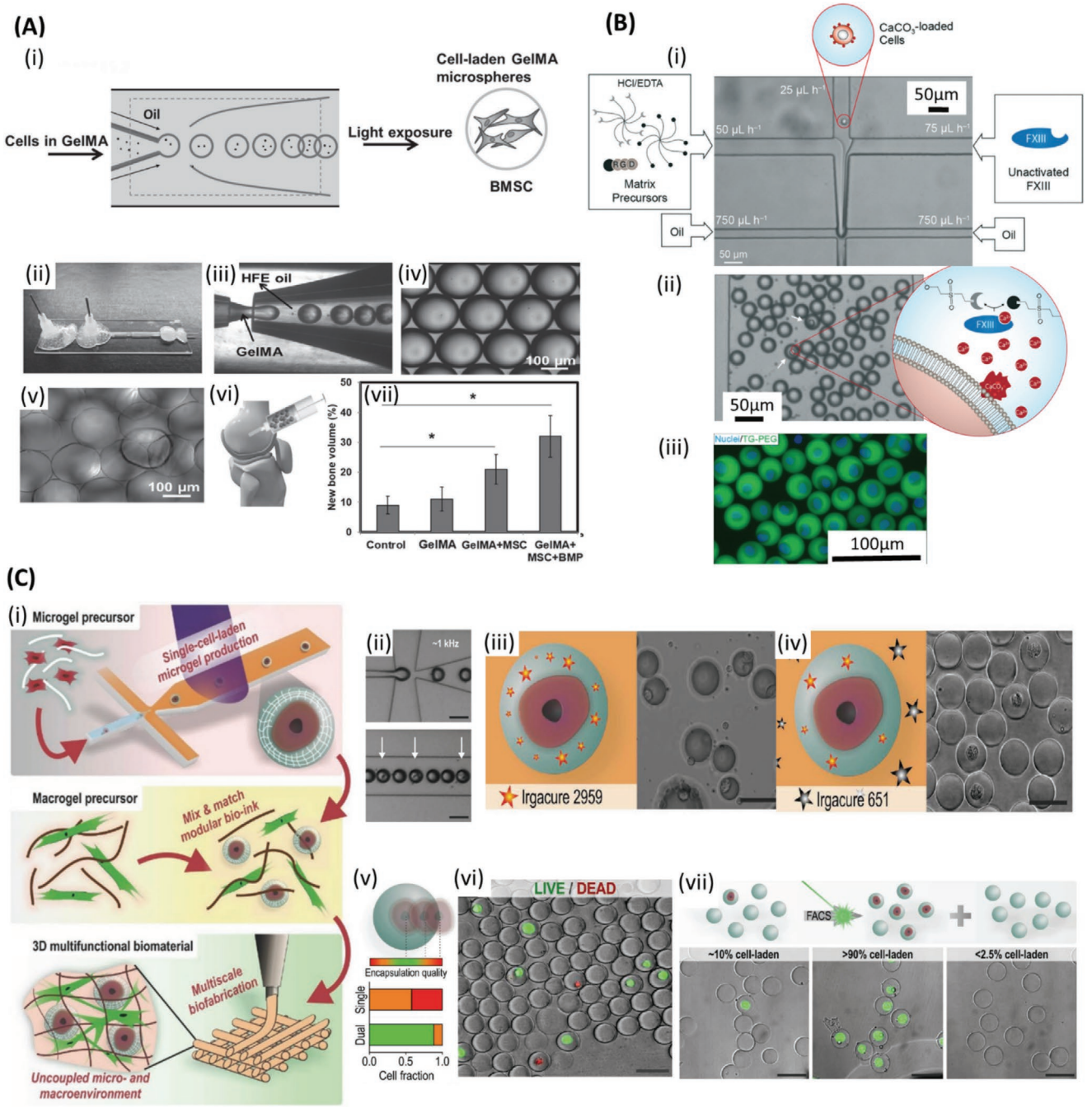

Figure 5. Microfluidic bioprinting of cell-encapsulated microspheres. A-i) Schematic of bone marrow derived mesenchymal stem cells (BMSCs)-encapsulated gelatin methacryloyl (GelMA) microsphere generation for bone regeneration. ii) Microfluidic device. iii) GelMA droplets formation. iv) Monodisperse GelMA microdroplets. v) Crosslinked GelMA microspheres. vi) Implanting the microspheres into the rabbit femoral defect. (vii) New bone volume (%) when implanting normal saline (control) and various contents of microspheres. Reproduced with permission.[299] Copyright 2016, Wiley-VCH. B) Selectively gelation of microniches: i) The process starts with injecting hydrochloric acid and ethylenediaminetetraacetic acid (HCL/EDTA) matrix precursors, diluted solution of $CaCo_3$-loaded cells and inactivated FXII into microfluidic chip, followed by jointing the solution in a laminar flow and shearing the fluid stream with the oily phase, resulting in monodispersed droplets. In the droplets containing $CaCo_3$-loaded cells, HCL dissolve $CaCo_3$ and realize Ca^{2+} ions that activate FXIII and results in on-demand gelation. ii) Droplets in the collection channel. iii) Fluorescent image of the cells (blue: nuclei). Reproduced with permission.[194] Copyright 2017, Royal Society of Chemistry. C-i) 3D multifunctional biostructures fabrication: Single-cell laden microgel formation followed by modular bioink preparation, and finally 3D bioprinting of multifunctional biomaterials with uncoupled micro- and macroenvironments. ii) Single cell encapsulation in polyethylene glycol diacrylate (PEGDA) precursor. iii,iv) Schematic and SEM images of failed and prosperous encapsulation using single and dual photoinitiator system, respectively. v) Cell encapsulation quality regarding the relative position of the encapsulated cells within microgel. vi) Live/dead staining of encapsulated cells (green: live; red: dead). vii) Flow cytometry-based sorting of the cell-laden microgels. Scale bars: ii–iv,vi,vii) 50 μm. Reproduced with permission.[186] Copyright 2017, Wiley-VCH.

various shapes, we will focus in the following sections on 3D printing of constructs that are formed by controlled deposition of objects to build multilayer complex structures.

3.3. Applications

3.3.1. Skeletal Muscle Tissue Engineering

Many studies have focused on the fabrication of 3D tissue constructs laden with myoblasts to mimic the native skeletal muscle.[50,196] In a study by Costantini et al., muscular tissue composed of myofibers was obtained by the use of coaxial microfluidic extrusion of muscle precursor cell-laden aligned fibrous constructs. Alginate and fibrinogen-PEG were used as bioink. The constructs were implanted in the subcutaneous tissue of immunocompromised mice to enhance the tissue maturation. The cells proliferated in the 3D printed fibers. By the time the biomaterial degraded, it was substituted by myotubes by 28 days post-implantation. The resulting myotubes showed high degree of alignment, similar to that of the native muscle tissue, while the myotubes formed in control bulk hydrogel were disordered and had entangled structure. It remains to examine such engineered tissue as a model for muscle tissue, e.g., for drug testing studies.[106]

3.3.2. Cardiac Tissue Engineering

Although numerous studies have attempted to develop native-like cardiac tissue constructs; developing novel bioinks and advanced fabrication techniques are required to circumvent current challenges in cardiac tissue engineering. Building heterogeneous 3D tissue constructs can be achieved by using low-viscosity bioink and microfluidic bioprinting.[161] Colosi et al. produced a 3 mm thick synchronously-beating cardiac tissue that was formed by seeding CMs into printed porous EC-laden fibrous construct.[111] The construct was formed by stacked layers ($n = 30$) of fibers (150–300 μm fiber-diameter) spaced by 200 μm forming an interconnected mesh. The layers were covalently-bonded together by using UV. The fibers were produced from alginate/GelMA by using a coaxial needle in the extrusion system coupled with combining Y-shape microchannel microfluidic device. Bioink (alginate, GelMA, photoinitiator, and cells) was fed into the internal needle and crosslinking solution ($CaCl_2$) into the external needle. The alginate prevented spontaneous gelation of GelMA and maintained low viscosity of the bioink. With this technique cell viability was 80%. In this method, the EC-laden construct was first cultured for 10 days. The cells were lined up at the periphery of fibers forming a monolayer. Afterward, the CMs were seeded and the construct started to beat after two days.

Because of the importance of vascularization of constructs intended for transplantation, Maiullari et al. developed a vascularized highly-oriented 3D cardiac tissue construct by using a high-resolution microfluidic bioprinting method.[105] They used ECs and induced pluripotent stem cell (iPSC)-derived cardiomyocytes (iPSC-CMs)-laden alginate and PEG-fibrinogen hydrogel as bioink. Vascularization was obtained from the proliferation of ECs along the printed fibers. In another paper, a uniformly beating endothelialized myocardium was obtained by using a coaxial microfluidic printing system.[107] The spontaneous beating started in the constructs after 48 h. in culture (50–70 min^{-1}) and it continued for 15 days. These beating constructs were formed by seeding with iPSC-CMs into the bioprinted fibrous structures (120 μm fiber diameter), which were subsequently cultured. The CMs showed various degrees of alignment in the scaffold. For bioprinting of fibrous constructs, Zhang et al. used a cell-laden mixture of alginate, GelMA, and photoinitiator (Irgacure 2959). The bioink was delivered through the core needle while the crosslinking solution ($CaCl_2$) through the sheath needle. The printed constructs were then kept in culture. It was found that alginate dissolved and leached out from microfibers in ≈5–10 days resulting in large pore formation, which enhanced cell spreading and proliferation. The ECs formed a confluent layer at the periphery of fibers by 15 days. Afterward, the ECs gradually broke off the fibers and migrated out during 33-day of culture. A vascularized cardiac tissue which is capable of beating for longer periods of time (up to 28 days) was produced by Zhang et al. by using microfluidic bioprinting method and two-step crosslinking.[197] First, EC laden GelMA alginate bioinks were printed into microfibers and crosslinked ionically. Then, UV crosslinking of the final construct was obtained. Endothelialized channels were formed after 16 days. A second cell type, neonatal rat CMs, was seeded into the space between the fibers. Although these studies represent important steps in the fabrication of vascularized and functional cardiac tissue, it remains to demonstrate the functionality of the vascular tree by testing for perfusion and integrity of vessels.[28,170] Subsequently, in vivo studies would be necessary to demonstrate the integration of formed vessels with those of the host and later their use as regenerative therapeutic modality in cardiac surgical models.

3.3.3. Tubular and Vascularized Tissue Engineering

Vascular networks have been integrated into engineered constructs to ensure their integration into the host tissues and function.[112,115,167,198] One approach for developing vascularized tissue is to use sacrificial approach materials, such as Pluronic F127,[170,199,200] sugar,[201] carbohydrate-glass,[202] agarose,[168,203,204] or gelatin.[205] Other methods can be achieved by SLA[11,206] or block assembly.[129] Pi et al. employed microfluidic bioprinting for the biofabrication of a multilayered cell-laden tubular tissue construct in a single step.[85] A coaxial nozzle system was utilized for extruding bioink constituted of GelMA, alginate, and PEG acrylate. This could be used to develop vascular tissues composed of SMCs and ECs, and also tubular urological tissues by using urothelial and SMCs (**Figure 6**A). Bioprinted tissues showed proper performance in terms of cell viability due to improving the fluid and nutrient supply.

Wadsworth et al. developed a contractile 3D bioprinted multilayer ring, the 3DBioRing, from an alginate-based bioink that contained primary human airway smooth muscle (ASM) cells (Figure 3x).[207,208] 2D models cultured in a standard well plate typically demonstrate a poor contractile response to agonists as a result of the low density of cells. However, 3DBioRing

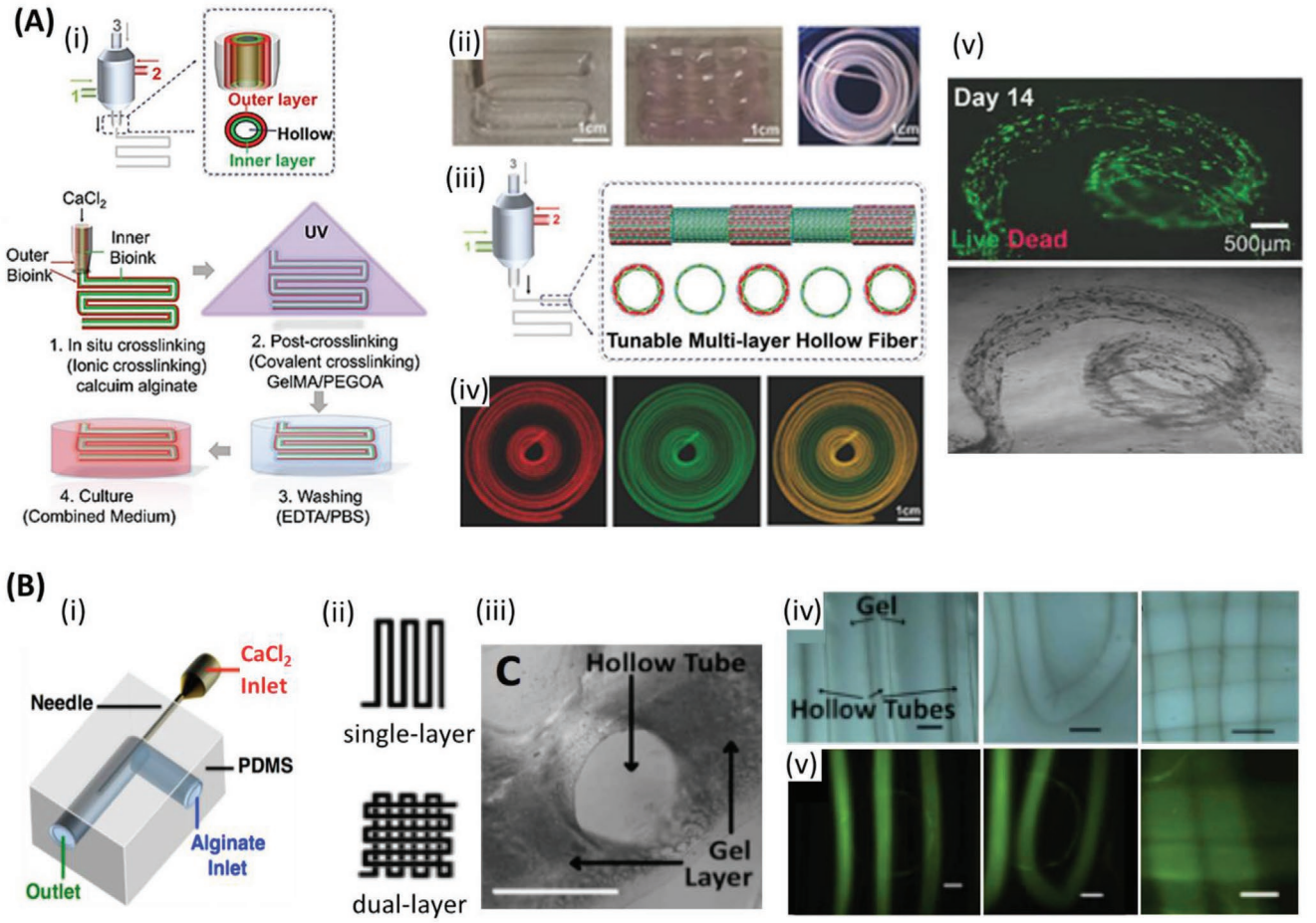

Figure 6. Microfluidic bioprinting of vascularized tissue. A-i) Steps followed for microfluidic bioprinting of multilayered tubular hydrogel constructs. ii) Images of bioprinted tubular constructs. iii) Fabrication of tunable single and double layered tubes. iv) Fluorescence images representing dynamic variation between single and double layered tube. v) Live/dead assay of human umbilical vein endothelial cells (HUVECs) and human smooth muscle cells (hSMCs) encapsulated within the tubes on day 14. Scale bars: ii,iv) 1 cm, v) 500 μm. Reproduced with permission.[85] Copyright 2018, Wiley-VCH. B-i) Coaxial microfluidic nozzle for hollow Ca-alginate filaments formation. ii–v) Continues gel layer with embedded single and dual layer channels. ii) Single and dual layer patterns. iii) Cross-section of the continues gel with embedded hollow channels. iv) Printed parallel straight channels (left), their arc connections (middle), and dual layer channels (right). v) Fluorescent images illustrating the nanoparticles flow along the channels shown in (iv), respectively. Scale bars: 1 mm. Adapted with permission.[187] Copyright 2016, SPIE.

(each roughly 1 cm in diameter, created with multiple layers of stacked ≈100 μm ionically crosslinked fibers) exhibited a dose-dependent contractile response when treated with histamine (EC50 of 0.6×10^{-6} M versus 2.7×10^{-6} M for human precision-cut lung slices (PCLS)) after 3 days of culture. Furthermore, they recovered through a dose-dependent relaxation response when later treated with salbutamol (EC50 39.3×10^{-9} M versus 40×10^{-9} M for human PCLS). The contractile rings were also placed in cryostorage for 48 hs and continued to show a comparable contractile and relaxation response. This demonstrated the potential to preserve 3D bioprinted tissues. Later, Dickman et al. extended the platform to intestinal and skeletal muscle tissues.[209] In a study by Selvaganapathy et al., it was demonstrated that perfused multilayer constructs have maintained cell viability, while this was decreased in nonperfused constructs. The constructs had channels that were formed by using coaxial bioprinting of EC-laden alginate structures.[187] The microfluidic nozzle had a needle embedded into the L-shape channel of the printhead. $CaCl_2$ was fed through the internal needle and bioink through the external microfluidic channel of the system (Figure 6B). This led to crosslinking of the inner surface of resulting tubules, while the outer parts of alginate were fused with parallel tubes. Readily perfusable channels were thus, obtained. It was also found that increasing flow rate led to increased fiber diameter. In another study, it was also possible to fabricate multilayered tubular constructs using a blend bioink composed of GelMA, alginate, and PEGTA to combine bioactivity, appropriate rheological properties, printability, and mechanical strength.[86] The structure was perfusable and could be maintained for 21 days. Stabilization of the resulting construct was achieved in 2-step procedure, first by fast ion crosslinking of alginate and then for permanent maintenance of shape by covalent photocrosslinking of GelMA and PEGTA. This technique, when used with needles of different sizes, produced various diameters and wall thickness. It should be noted that thick walls may compromise reaching oxygen and nutrients to cells, while thin walls may not be mechanically stable or have sufficient room for cells. Thus, a nozzle having an external

needle size of 20 G and an internal needle of 30 G was used to produce vessels having an outer diameter of 800 mm and a wall thickness of 110 mm. Alginate was removed by ethylenediaminetetraacetic acid EDTA. Constructs having up to 10 layers and having a size of $9 \times 8 \times 7$ mm, were bioprinted. The constructs were subsequently incubated in culture. Cell viability was >80% at 1, 3 and 7 days of culture for the constructs crosslinked with UV light exposure times of 20 and 30 s. The ECs and MSCs contained in the bioprinted constructs spread and proliferated, and they reached confluence, filling the wall and forming an integrated vessel-like structure after 21 days in culture. After 21 days, mechanical instability of vessels due to polymer degradation and thin walls was observed. Although this new technique is better than conventional microfabrication or sacrificial templating approaches that were used for producing perfusable vascular structures, designing better bioinks is required in order to produce vessels with more stable mechanical properties, which can be maintained for longer periods of time.

3.3.4. Osseous and Chondral Tissue Engineering

Microfluidic bioprinting can be implemented to fabricate tubular microfibers with double layers comprised of a thinner inner layer and a thicker outer layer that mimic the osteon nature. A microfluidic chip was used by Wei et al. to produce complex 3D structures composed of cell-laden microfibers.[210] Utilizing ionic and UV crosslinkable methacrylated alginate offered both structural integrity and biological activity to the 3D constructs. Osteon-like hollow double-layer fibers for bone tissue engineering were obtained. They had an outer layer loaded with osteocytes for bone regeneration and the inner layer loaded with ECs for vascularization. In another study, Liu et al. formed cell-encapsulated microfibers that mimic the osteons using a double coaxial microfluidic device.[211] They developed a bioink of alginate/GelMA/alginate lyase that could be degraded over time while keeping the integrity of microfibers in the initial stages of the printing. The microfluidic device consisted of three inlets to build the double layer tubular microfiber. HA injected into the 1st inlet (the channel in the center of the microfiber) shaped the tubular form of the fibers, while cell-encapsulated alginate/GelMA injected through 2nd and 3rd inlets shaped the middle and outer layers of the tubular microfibers. The double-layer tubular microfibers were laden with MG63 and HUVEC in the outer and middle layers to mimic the cell distribution of the osteon. Gradual degradation of alginate was found to facilitate cell aggregation and proliferation due to more room created following the degradation of the hydrogel. Cell aggregation diameter was increased from 37.9 to 72.5 μm and from 34.8 to 62.5 μm (after 7 days of culture) for MG63 and human umbilical vein endothelial cells (HUVECs), respectively. Recently, microfluidic bioprinting has been used to create heterogeneous constructs for the regeneration of full-thickness chondral region. In this study, Idaszek et al. have fabricated graded hydrogel scaffolds in which human mesenchymal stem cells (hMSCs) and human articular chondrocytes (hACs) have been precisely compartmentalized mimicking the chondral region, i.e., calcified and hyaline cartilage—presents in the joints.[172] The extrusion system consisted of a microfluidic device bearing a Y-junction downstream connected to a passive serpentine-based mixing unit compatible with multimaterial/multicellular deposition and rapid switching/mixing among two different bioinks. By exploiting such an extrusion system in combination with instructive bioinks mimicking the composition of the different zones present in the native articular cartilage, the authors showed an in vitro heterogeneous differentiation of hMSCs within a single construct that partially recapitulated the native chondral region when tested in vivo.

3.3.5. Fabrication of Organoids

The use of microfluidics enables also the building of organoids.[212] Organoids were developed by coculturing pluripotent and adult cells with matrix and biomolecules, and they were found to have autonomous self-assembly.[213] Yamada et al. used microfluidic channels (50 mm long and 160 μm deep) to control precise positioning of hepatocytes and feeder fibroblasts in alginate microfibers.[188] Subsequent culture and alginate removal using alginate lyase led to the formation of scaffold-free hepatic microorganoids (1 mm long and ≈50 μm diameter) that resemble hepatic cords. High cell viability of ≈80% over 30 days was observed. Significantly enhanced liver function was seen up to 90 days, as compared to monoculture and single cultivation (without fibroblasts) in hydrogel fibers (**Figure 7**).

3.4. Limitations

One of the challenges with the use of microfluidic 3D bioprinting is the difficulty to maintain precision, especially at the corners of resulting constructs because of the difficulty in maintaining smooth nonfluctuating flow and pressure in the device.[184] Thus, careful design of hardware and bioinks is required.[214] Cell viability during the microfluidic bioprinting can be affected by different factors, among which a key factor is the amount of shear stress applied to cells.[215–217]

In addition, management of the sheath fluid for larger models can also be challenging. To solve this issue, volatile fluids (e.g., perfluoro (methyldecalin (PFD)) are used in literature.[218] In this case, the volatile sheath flow evaporates just after dispensing from the nozzle due to the high vapor pressure. In addition, flow instability may occur that disturb the printing process when the sheath flow is quite larger than the core flow (bioink). Thus, using the proper size of the nozzle for bioink and sheath flow is of great importance. Other than sheath flow, crosslinking by exposing the construct to the UV light or printing in a $CaCl_2$ bath can also be performed for some cases. However, these crosslinking techniques may be challenging for printing tall constructs. Although using PDMS printheads in microfluidic 3D bioprinting has eased the process, however there are some limitations. Using PDMS printheads is limited to low extrusion pressures since the flexibility of PDMS.[218] One other issue with PDMS-based systems is their tendency to absorb small molecules making it difficult to control the chemical environment precisely. In addition, fabricating PDMS microfluidic chips may require the use of multistep photolithography processes that can be challenging and

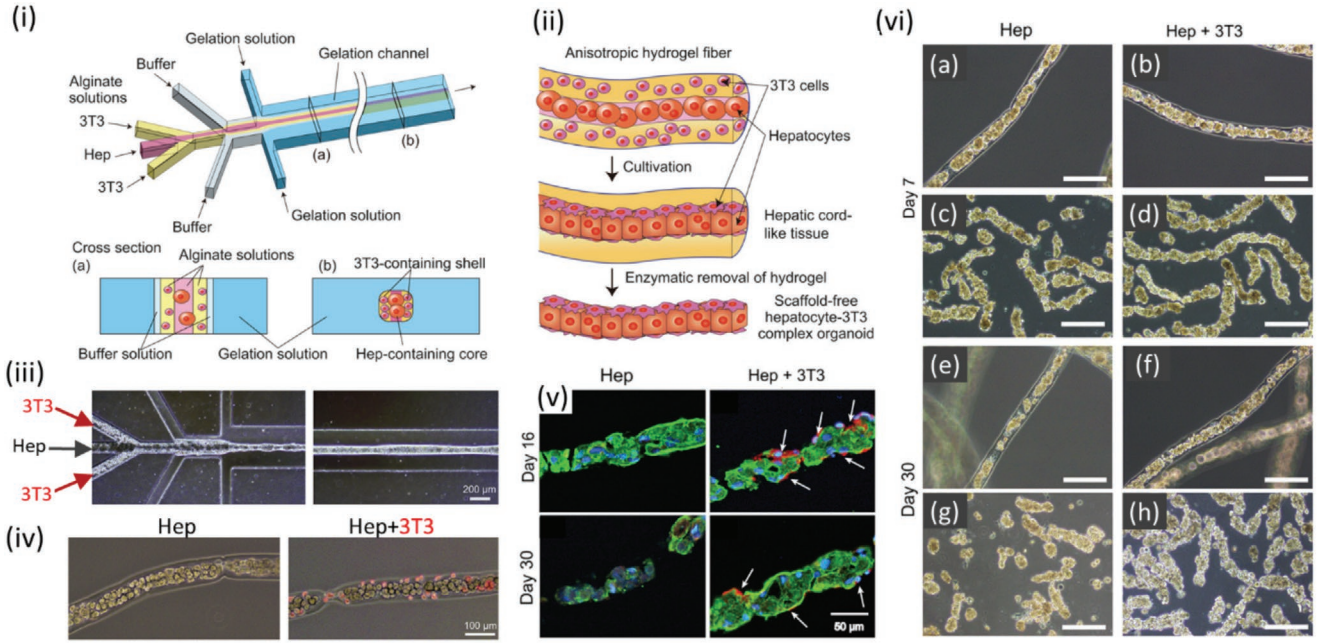

Figure 7. Microfluidic bioprinting of organoids. i) A microfluidic device for generation of sandwich-structured alginate microfiber with hepatocytes and 3T3 cells layers. ii) Formation process of scaffold-free hepatocyte-3T3 complex microorganoid. iii) Hepatocytes and 3T3 cells-encapsulated hydrogel microfibers formation by microfluidic device. (iv) Micrographs of hepatocytes in microfibers with and without presence of 3T3 cells. v) Double-immunofluorescent staining of hepatocytes-encapsulated microfibers with and without 3T3 using CK18 (green) and vimentin (red) antibodies (green: hepatocytes; red: 3T3). vi) Production of hepatic microorganoids in alginate microfibers: without 3T3 after a) 7 and e) 30 days, and with 3T3 after b) 7 and f) 30 days. Enzymatic digest of the alginate microfibers and hepatic microorganoids recovery for the microfibers: without 3T3 after c) 7 and g) 30 days, and with 3T3 after d) 7 and h) 30 days. Scale bars: iii) 200 µm, iv) 100 µm, v) 50 µm, and vi) 200 µm. Reproduced with permission.[188] Copyright 2012, Elsevier.

time-consuming. One of the constraints of microfluidic 3D bioprinting is the low throughput that can be compensated by the parallel usage of several chips.[219] In addition, it is tough to scale up the microtissues and organoids fabricated by microfluidic 3D bioprinting. Thus, the constructs have smaller sizes than the actual human tissue.[220] Microfluidic bioprinting is limited to low viscose bioinks to decrease shear stress.[221] However, microfluidic bioprinting of the fairly high viscose bioinks with shear-thinning behavior was recently reported.[222] The dispensed material should be crosslinked at the very end of the nozzle to avoid clogging issues; however, there still exists a risk of clogging due to low flow rate of bioink, highly concentrated bioink, diffusion of crosslinking bath into the nozzle (for the cases that 3D printing occurs in the crosslinking bath), etc.[84,92] Either the cells, the extracellular matrix, or crosslinked bioink can clog within the channel pathways. For instance, microfluidic printheads designed for mixing a prepolymer solution with a crosslinker are prone to early crosslinking within the fluid pathway, which can damage the printing system. In addition, control of temperature for thermoresponsive hydrogels is hard since the channel may expand in higher temperatures. Thus, many challenges and limitations remain when 3D microfluidic bioprinting of complex heterogeneous constructs.

3.5. Recent Advances

3D bioprinting of multiple bioinks or cell types is necessary to generate functional constructs that mimic the actual tissues/organs.[223] In addition to the cell types and chemical compositions, the mechanical properties and permeability of the 3D printed constructs can be gradiently programmed to mimic the target tissues/organs.[224–228] For instance, osteochondral scaffolds 3D printed with a gradient transition of porosity and ceramic content mimic human trabecular bone better than uniform scaffolds in terms of compressive properties.[229] Simultaneous compilation of multiple types of gradients in material composition, cell type, density, and architecture supports the development of the next generation tissue regenerative scaffolds. Multimaterial bioprinting can be done by using either separate independently controlled printheads, or one printhead, while a selector valve switches the bioink on demand during the printing process.[135,170,230,231] Fast and smooth switching between various bioinks in a precise manner is the key challenge in multimaterial 3D bioprinting techniques. Printing using a single printhead is faster[212] than with the use of multiple printheads.[188,190,232] Using multiple separate printheads is a slow process. Alternatively, the use of microfluidic channels allows programmed switching between different inks,[80,214] to achieve sequential or simultaneous extrusion of different materials[80,111,170,184] (Figures 3 and 8A) or cell types[112] (**Figure 8**B). In addition, microfluidic printheads were combined with extrusion printing. The opening and closing periods of the valves define the extruded length of each bioink.[171] Microfluidic valves that enable high-speed opening/closing of the channels are required for multimaterial microfluidic bioprinting of complex-shape heterogeneous constructs. The precise control of the flow rate for the bioinks with various viscosities can also be quite

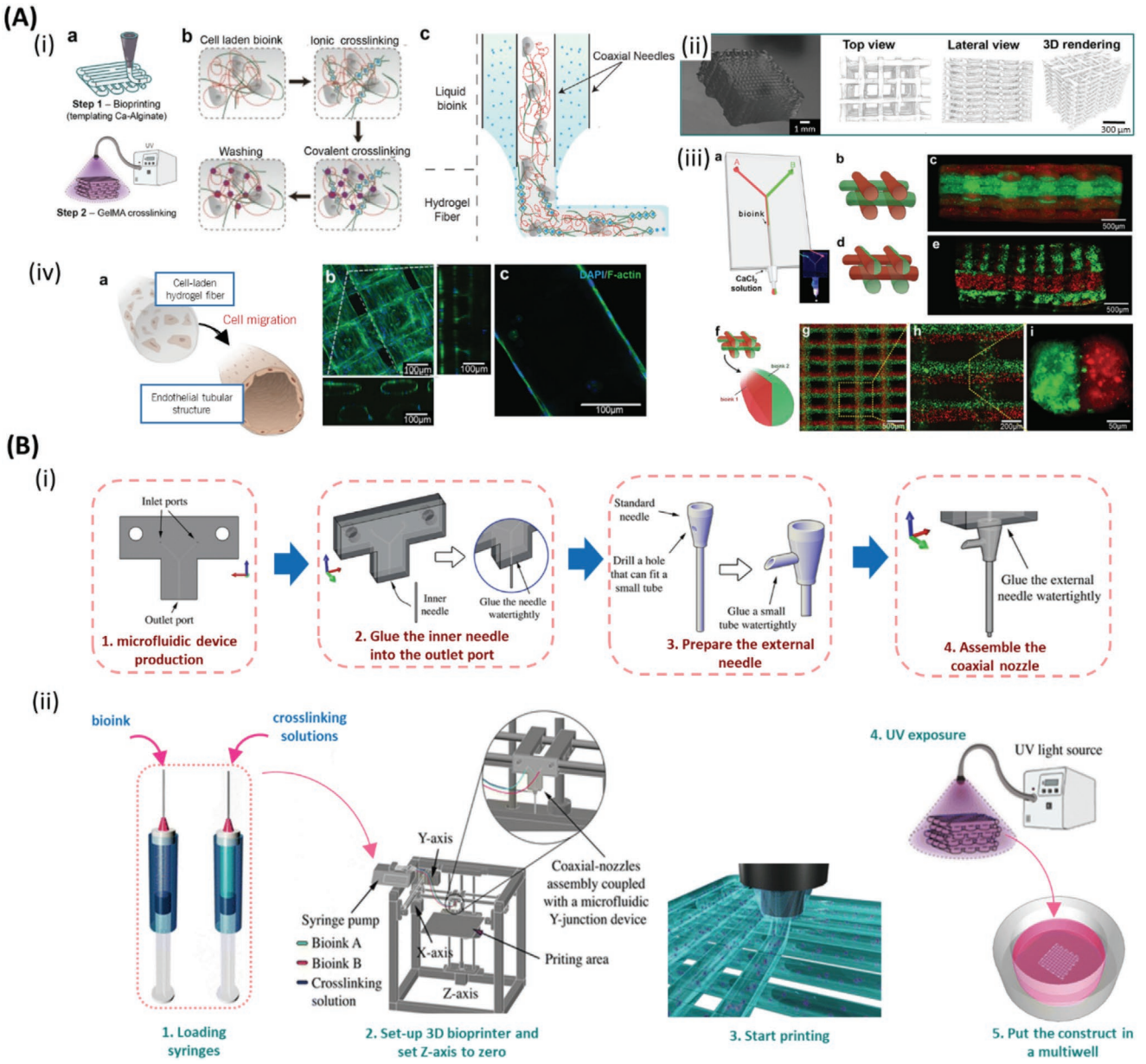

Figure 8. Multimaterial bioprinting. A-i) Fabrication process of 3D cell-laden constructs: a) Layer-by-layer bioprinting of 3D constructs along with two steps of crosslinking. b,c) Bioink consisting of gelatin methacryloyl (GelMA), alginate, photoinitiator, and cells are extruded through inner nozzle, while CaCl2 flows through outer nozzle resulting in ionically crosslinking of alginate followed by ultraviolet (UV) light crosslinking of GelMA. ii) Final 3D construct and μCT reconstructions. iii) Multimaterial bioprinting using a microfluidic chip for developing constructs made of two separate bioinks: b,c) alternatively, d,e) alternate and simultaneously, and f–i) simultaneously extrusion. Red and green colors in the fluorescent images present two separate bioink extruded through Y-shape channel of a coaxial needle. iv-a) Schematic of the bioprinted microfibers before and after the migration of the encapsulated human umbilical vein endothelial cells (HUVECs) to the outer regions of the microfibers after 10 days of culture. Confocal microscopy images of the tubular microfibers: b) top, and c) cross-sectional view. Scale bars: iii-c,e,g) 500 μm, h)200 μm, i) 50 μm, and iv) 100 μm. Reproduced with permission.[111] Copyright 2016, Wiley-VCH. B-i) The fabrication procedure of a microfluidic printhead; ii) Schematic of the microfluidic printhead integrated with a customized bioprinter for multimaterial/multicellular bioprinting of cell-encapsulated scaffolds followed by UV light curing. Reproduced with permission.[112] Copyright 2017, Springer Nature.

challenging.[230] One other serious consideration in multimaterial 3D bioprinting is the risk of crosscontamination between the various materials especially when a single printhead is used.[22] Gradient compositions may also be obtained by the active mixing of different bioinks in various ratios that gradiently changes through the 3D printed construct. Microfluidic bioprinting allows for efficient mixing,[192] easy deposition of multiple materials and gradient building in the resulting construct. In an interesting work, Ober et al. developed a microfluidic printhead, having an embedded rotating impeller to actively mix multiple inks (**Figure 9**A).[192] In earlier reports on cell–laden microfibers, it was anticipated that the assembly

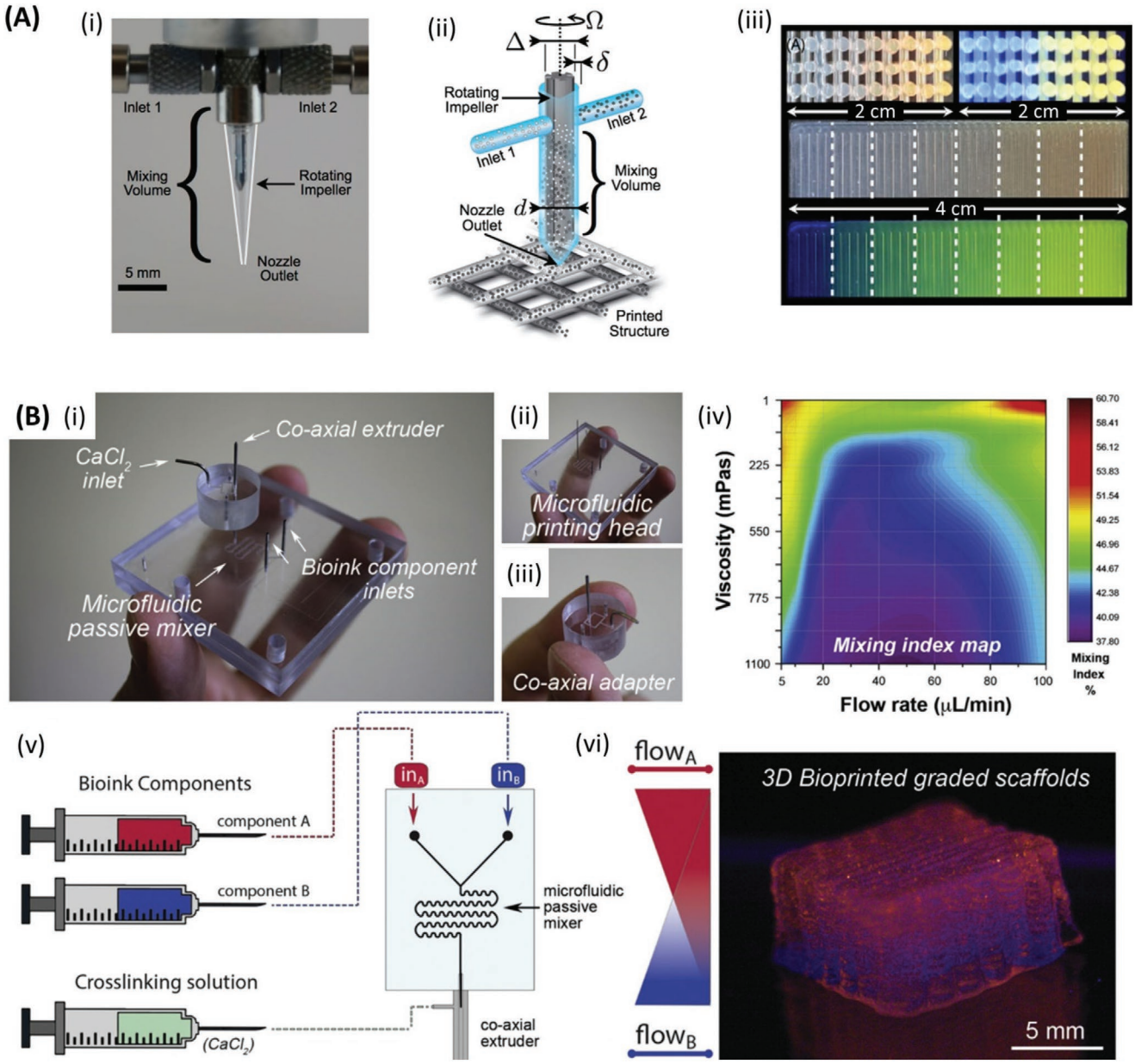

Figure 9. Graded structure bioprinting. A-i) Optical image of an impeller-based mixer. ii) Schematic of a mixing nozzle for active homogenization of two inks entered through inlets #1 and #2 for 3D printing of constructs of multiple materials. iii) Cross-section images of 3D lattice constructs showing the continuous variation of the fluorescent pigment concentration under bright light (top left) and UV light (top right). 2D structures showing the discrete variation of fluorescent under 8 different mixing ratios under bright light (middle), and UV light (bottom), respectively. Scale bars: i) 5 mm. Reproduced with permission.[192] Copyright 2015, American Physical Society. B-i) Microfluidic extrusion system composed of ii) the microfluidic printing head and iii) the coaxial adapter. iv) Mixing index heatmap is shown. v,vi) The schematic of the fabrication process and the final 3D bioprinted graded scaffold are shown, respectively. Reproduced with permission. [172] Copyright 2019, IOP Publishing.

of multiple fibers having one or different types of cells will enable the engineering of complex tissue constructs.[233] Idaszek et al. developed a multimaterial microfluidic bioprinting system for either separate or simultaneous deposition of bioinks to generate the constructs with heterogeneous properties by zonal programming of the composition and microstructure.[172] Mixing various bioinks was enabled by designing a passive mixer in the microfluidic printing head connected to the coaxial extruder (Figure 9B). A gradient of compositions and cells, mimicking various regions of human articular cartilage, represented a gradient transition from hyaline to calcified cartilage. A unidirectional gradient of hMSCs was achieved by encapsulating the cells in zone-specific bioinks and it was further confirmed that coculture of hACs and hMSCs improved chondrocyte proliferation and the quality of the hyaline cartilage. Thus, multimaterial 3D microfluidic bioprinting platforms can be utilized for generating scaffolds that mimic complex-shape tissues/organs such as osteochondral, osteotendinous, myotendinous,

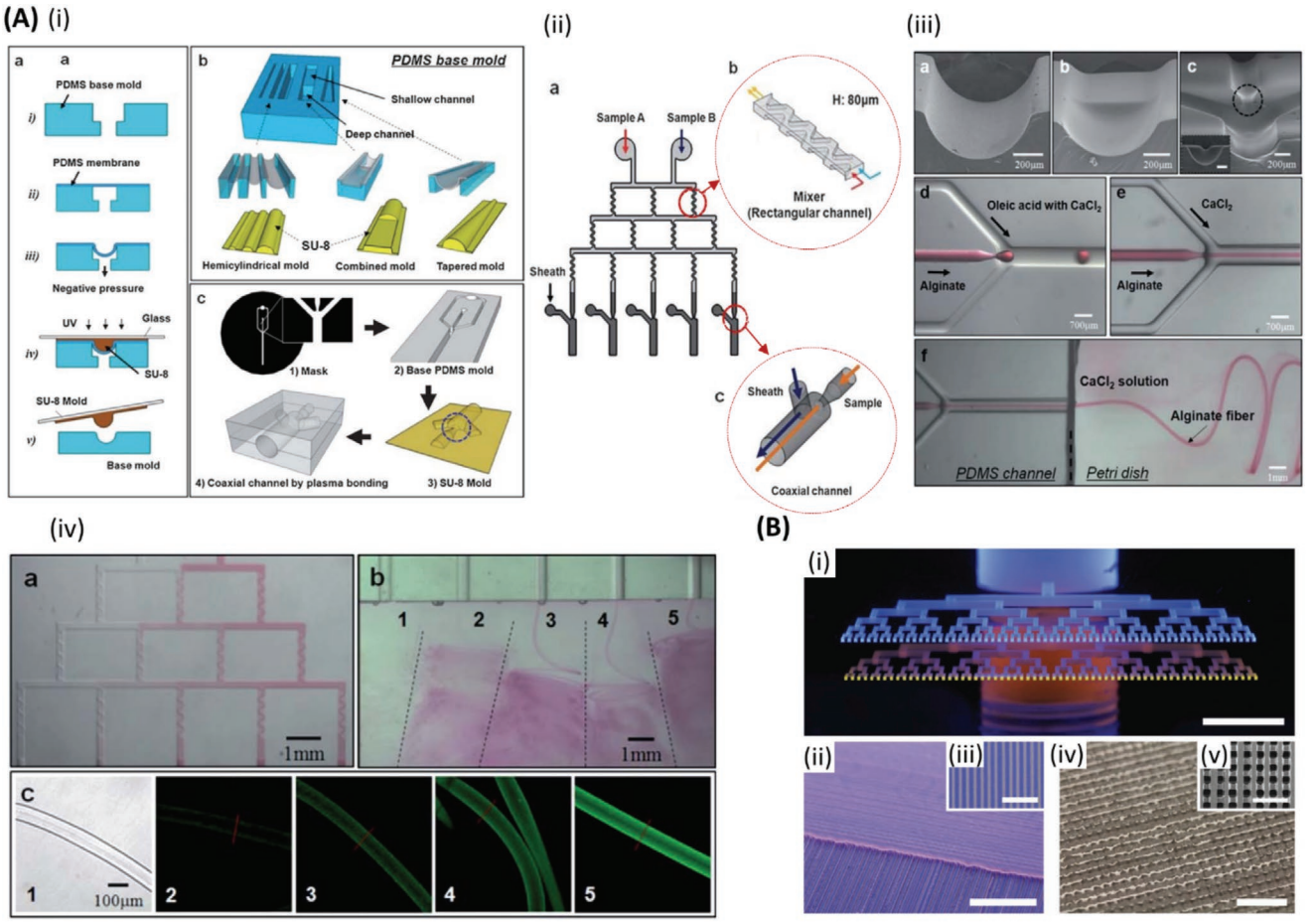

Figure 10. High-throughput microfluidic bioprinting. A-i) Schematic of the fabrication process of the coaxial microfluidic chips. ii) Schematic of the platform for a) high-throughput printing of fibers with various compositions employing several b,c) micromixers and coaxial flow channels with separate inlets for sheath flow. iii) SEM images of a–c) hemicylindrical, rectangular and cylindrical combination, and hemi-coaxial-flow channels, respectively. d,e) Microdroplets and continues flow formation through the coaxial-flow channels, respectively. f) Alginate microfiber formation through coaxial-flow channel. iv-a) Generation of a stepwise gradient in the fluid passing the channels with in-line micromixers, b) high-throughput production of microfibers, and c) optical and fluorescence images of fluorescein isothiocyanate tagged to bovine serum albumin (FITC-BSA)-immobilized fibers fabricated through various channels. Scale bars: iii-a–c) 200 μm, d,e) 700 μm, and f) 1 mm and iv-a,b) 1 mm and c) 100 μm. Reproduced with permission.[189] Copyright 2010, Royal Society of Chemistry. B) High-throughput multimaterial printing through dual hierarchical microvascular multinozzle printhead: i) optical image of the printheads filled with blue (inlet above) and yellow (inlet below) inks. ii,iii) Optical images of multilayer construct of blue and yellow wax filaments. The magnified image represents a single layer construct. iv,v) Optical images of the printed construct out of wax filaments infilled with a photocurable epoxy resin. The magnified image shows the cross-section of a 10-layer 3D construct after removing the sacrificial wax. Scale bars: i,ii) 5 mm, iii,iv) 2 mm, and v) 1 mm. Reproduced with permission.[234] Copyright 2013, Wiley-VCH.

and neuromuscular tissues, where precise transient composition is needed. It is also possible to simultaneously produce multiple fibers, each having different composition by using coaxial microfluidic channels (**Figure 10**A).[189] High-throughput printing of single and multiple materials was possible by using a multinozzle array composed of microvascular network. It is also possible to simultaneously print different materials by having dual printhead, each fed with different material. The use of this system will result in dramatic reduction in printing time, e.g., to print a 3D construct using single-nozzle printhead that takes a day, will take only 22 min by using 64-nozzle printhead system. It was also suggested that the system can be used for producing cellular 3D constructs (Figure 10B).[234] The use of microfluidic 3D bioprinting systems enables more efficiently building of heterogeneous 3D tissue constructs.[161] For example, Colosi et al. used a coaxial needle in an extrusion system that was coupled with microfluidic device to produce alginate/GelMA fibers containing aligned HUVECs and CMs (Figure 8A).[111] Coaxial printing to produce core–shell constructs is especially useful when the material of the core and the shell may need different processing parameters. Active mixing of the inks at the printhead enables us to obtain homogenous bioink[192] that allows also for building desired gradients in the resulting construct.[212]

4. Printing Parameters and Promises in Bioprinting

Several studies have examined the effect of printing parameters on different aspects of the 3D printed structures from fidelity

to the final physical properties.[235,236] This is important in a sense that the formation of pores in the scaffolds plays a vital role in the successful seeding of the cells within the bioprinted structures and this entails a high printing fidelity due to the small scale of the optimal pore sizes and internal features. The structural integrity of the macro/microfeatures circumvent the need for compensation procedures to be implemented during the design process. Proper understanding of these parameters and their optimization can improve the accuracy of the printed scaffold resulting in a better recapitulation of the target native tissue.[237] In the extrusion-based and microfluidic-assisted bioprinting technologies, the printhead size and printing speed directly influence the size of the deposited fiber and overall accuracy, fidelity, mechanical properties, and porosity of the fabricated scaffold. These parameters are synergistically coupled with the bioink properties such as viscosity to attain an optimized printing process. Optimization of these parameters is essential for having high resolution in the printed structure. When it comes to bioprinting living cells, the range of printing parameters becomes limited to maintain the cellular activity of cells (i.e., cell migration and proliferation). Post printing viability of the cells has been well tuned by manipulating the structural features such as porosity in the printed tissue constructs. Besides, the scaffold stiffness, which is known to play a vital role in regulating cell behavior in the ECM, is locally controllable by the architectural features and internal pore shape design.[237–239]

Bioprinting speed, which can be controlled through the applied pressure, imposes a significant influence on the resolution of the bioprinted structure due to the changes in the deposited fiber diameter. These parameters need to be adjusted based on the bioink properties and viscosity.[197] Also, higher bioprinting speed and pressure are associated with higher shear stress levels applied to the cells which is unfavorable for maintaining cell viability.[240] Proper viscosity of the bioink is of great importance for both extrusion and microfluidic bioprinting processes. The low viscosity of the bioink diminishes the structural fidelity and high viscosity may result in nozzle clogging. Extrusion-based bioprinters are able to 3D print bioinks within the range of 30 to 6×10^7 mPa s. On the other hand, the bioink viscosity affects the shear stress level that is transferred to the encapsulated cells. Nozzles with larger diameters operated with lower pressure levels were introduced as ways to reduce the shear stress.[237,239,241,242]

4.1. Cell Viability in Microfluidic Bioprinting

Translation of 3D printing technologies that were initially adapted for materials such as metal and polymers to the bioprinters dealing with living cells and biomolecules entails the use of biocompatible procedures that are thoroughly cell-friendly. Many efforts have been made to solve this problem by replacing the 3D printing elements with components performing under mild conditions for bioprinting. This process involves avoiding high temperatures and aggressive solvents that are not compatible with cells and more importantly developing bioinks with different properties and integrity that possess excellent properties for the bioprinting for encapsulating various cell types.[243,244] Bioinks can have a significant effect on cell viability in 3D bioprinting by promoting cell proliferation, differentiation, and interaction in the bioprinted structure. The requirements such as printability, mechanical integrity, biocompatibility, and biomimicry ability are among the important properties that should be met when choosing or designing the appropriate bioink materials.[244] The parameters of bioink should be optimized considering the target tissue and its properties, cell type and density to obtain desirable 3D structure. Mechanical integrity of the bioink plays an important role since the bioink should be able to support the cells during and after the printing process and be formed to the desired 3D shape without any defects or collapsing. In addition, the permeability and diffusion properties of the bioink will determine the transport of oxygen and other essential materials to the cells. One way to address this issue is to incorporate oxygen releasing materials such as hydrogen peroxide, sodium percarbonate (SPO), and calcium peroxide (CPO) within the printed tissue construct.[245] To investigate the effectiveness of oxygen releasing material on maintaining cell viability, Oh et al. studied the effect of CPO particles incorporated into the PLGA scaffold to generate oxygen for the 10 days period, which resulted in a significant increase in cell viability and growth.[246] In another study, Khorshidi et al. fabricated CPO nanoparticles and incorporated them in PLGA microparticles to enhance control over oxygen releasing of this material.[247]

Appropriate bioinks can promote cell tissue interaction and cellular activity. Another important aspect of bioinks is the biomimicry ability of bioink that has a vital role in cell attachment and activity. Biomimetic materials are able to control the cellular interactions by binding the receptor to the ligands that are present in the bioink. This affinity between ligand and receptors can determine many factors in cell activity, attachment, and migration. Therefore, biomimicry is one of the important parameters for the design of bioink and materials for bioprinting and cell viability.[237–239,242,248] Bioinks can be categorized as natural and synthetic according to their synthesize approach. Natural bioinks such as alginate, gelatin, collagen, agarose, hyaluronic acid, silk fibroin, and ECM are derived from natural sources and generally show cell biocompatibility. Synthetic bioinks are developed by chemical synthesis of materials which are usually controllable processes. They can be manufactured with desirable mechanical and crosslinking properties which thrive them for fabrication fine structures. However, compared to natural bioinks, they can induce more cytotoxicity.[238] The shear stress experienced by the cells during the printing process is one of the primary challenges present in the viability of bioprinted products. Modulating the shear stress can directly change the cell environment and facilitate high cell viability.[249,250] Desirable shear stress can be achieved by manipulating parameters such as nozzle diameter, the viscosity of the bioink and applied pressure. In microfluidic-based bioprinters which normally work with lower viscosity bioinks, the flow rate plays a crucial role in shear stress applied during bioprinting process. Shear stress level produced in microfluidic printheads is less than extrusion dispensers. Therefore, multiple considerations should be taken to account in order to ensure high cell viability in microfluidic-based bioprinting platforms [181,249,251]

4.2. Extrusion and Microfluidic Bioprinting versus Other Techniques

Extrusion-based and microfluidic coupled extrusion systems have brought a great promise to the field of bioprinting as they can integrate a wide range of materials and polymers with different crosslinking mechanisms. Printheads with microfluidic devices enable higher resolution in extrusion-based systems. Spatial gradients can be functionally made within the extruded fiber in a controllable manner. 3D shaped structures made of microgels with sophisticated structures is advanced since the advent of microfluidic mediated bioprinting. However, the printing resolution can be lower compared to some of the printing techniques (particularly those of optical basis). For instance, the printing speed and resolution is higher in the inkjet bioprinters compared to the extrusion-based techniques involving those with microfluidic coupled printheads. They have also shown relatively greater cell viability. However, inkjet bioprinters are limited in terms of the viscosity of the inks that they can handle. It is reported that the inkjet printers regularly deposit the inks with a viscosity about 15 mPa s^{-1}.[252–254] Bioinks with high cell density are not printable, both from a viscosity and clogging perspective. However, inkjet bioprinters can be used for single cell printing. In addition, the printhead motion is usually faster with inkjet bioprinters but the volume flow rate of the extrusion-based approaches is much higher, so ultimately inkjet bioprinters can make smaller more precise structures faster but not larger ones.

Laser-assisted bioprinters, on the other hand, are capable of printing materials at high speeds (scanning speed of ≈2000 mm s^{-1}). Promising cell viability results also confirm their potential for the fabrication of artificial tissue constructs. However, the printing matrix materials are usually limited to those of photocurable polymers. Other drawbacks for this type of bioprinters are the relatively high cost of printing and high preparation time.[238,255] SLA bioprinters can print at the high speeds and have shown no limitation on the rheological properties of the bioink.[256] In addition, high cell viability, high resolution, and printing fidelity are the other advantages of SLA technology. However, the complexity of the printing procedure along with the need for photosensitive bioinks are the limitations of this process.[238] Low cell yield (proportion of the cells that end up in the printed model) is a drawback of SLA since a large proportion of the cells are unused in the uncrosslinked bioink.

5. Current Challenges and Future Perspectives

Microfluidics-based bioprinting is associated with challenges that include the precise positioning of cells and materials in appropriate locations to generate accurate constructs that recapitulate the native tissues structure and function. The ability to achieve desired resolution while maintaining the functionality of printed cells could be difficult. Additionally, working with pluripotent stem cells imposes additional challenges as it is hard to print these cells with high levels of viability while maintaining their differentiation potential. In addition, differences exist when producing these microfluidic devices, which can lead to variability during the printing process and suggesting a need for closed-loop control in future systems. It is also important to maintain precise control over the pressures and flow rates being used to deliver and mix the bioink, its crosslinker, and the cellular components. Accordingly, various technologies need to be developed for addressing these challenges.

Several studies have combined microfluidics with 3D bioprinting (extrusion bioprinting) to generate different tissue constructs, including vascular conduits and muscle tissues.[88,106,131] Other benefits of using microfluidic-based bioprinting include the ability to generate constructs with better vascularization that would help cell growth and differentiation.[257] Such technologies can also enable the deposition of cells in defined areas to create physiologically relevant structures, such as myofibers.[106] Such strategies could be applied to engineer other tissues, such as nerves where cellular alignment influences tissue functionality. Moreover, the technique can be applied to develop complex tissues along with the necessary vasculature, which will represent a major advance over current approaches. Furthermore, printed constructs can also be incorporated into organ-on-a-chip devices and their use in physiological, disease modeling, and drug testing can be developed.[258] Applications in drug release and replacement therapy such as in the case of diabetes and other endocrine functions/organs will further expand in the future. Moreover, the food industry in the future may benefit from these advances by bioprinting food products, such as cultured meat in the lab.[259] Such methods would provide a sustainable source of food in comparison with current farming practices.

Another area for the further improvement of the 3D printing represents the development of novel bioinks with unique features that enable them to respond to changes in their environment. Such materials can respond to changes in temperature, pH, and other conditions, and these technologies will need to be adapted to generate printable formulations. Microfluidic-based 3D printing can employ stimuli-responsive materials[260–262] to produce dynamic and 4D constructs for drug delivery tissue engineering and actuator products.[261]

One of the long-term goals of 3D bioprinting is the ability to produce clinical-grade tissues.[263] However, translation of these 3D printed implants[173] and tissues to clinical applications will require long-term in vivo testing to investigate the functionality and integration of constructs. The performance of these bioprinted 3D constructs must be evaluated in appropriate preclinical models of diseases and defects to demonstrate the feasibility and efficacy of this new therapy. Examples may include the application of bioprinted constructs as skin grafts.[264]

3D bioprinting of iPSCs has also been successfully achieved by using novel microfluidic bioprinting technologies.[251,265] Microfluidic-based bioprinting of these cells will enable further the development not only of customized constructs but also allows for advancing future personalized medicine in which constructs can be used for devising therapy and prescribing appropriate medicines in effective dosage using a patient's own iPSCs. The application of the microfluidic-based approaches has yet to be studied for a wide range of organ and tissue types such as skin given the potentials in precisely engineering the materials and biomolecules. The integration of sensors and data communications,[266–269] to current systems will enhance the control of the bioprinting process as well as functional control of resulting tissue grafts to provide an essential part of the cycle of therapy in future.[270]

6. Clinical Translation of 3D Bioprinting

3D bioprinting is an emerging method that has the potential to develop the next generation of tissue constructs to serve as models for drug development or to use as implants for regenerative medicine. Although 3D bioprinting has significantly improved tissue engineering capabilities, there still exist some challenges to tackle before the wide and clinical translation of this technology. One of the main challenges that remains to be addressed is the robust fabrication of tissues in a larger scale. The number of cultured cells as reported in published works is somewhat limited and thereby scaling the fabrication process is challenging. Recently, protocols compatible with good manufacturing practice (GMP)[271] and robotic systems[272] have been developed for large-scale growth of bone marrow-derived stem cells. Robust, large-scale, and consistent fabrication of tissue constructs may be further facilitated by combining deep learning with 3D bioprinting techniques and implementing proper feedback systems to optimize the tissue manufacturing process. Health 4.0 has recently revolutionized the manufacturing units as it can form a self-training platform that uses big-data generated through the manufacturing process to enhance the fabrication outputs.[273–275]

Despite the fact that 3D printing has, to some extent found its way to the clinical practice,[263] we are still way far from the wide translation of 3D bioprinting for solving biomedical problems. 3D printing has been already used for rapid prototyping of damaged tissues from the stack of micro-CT images taken from patients for the sake of surgical training as well as surgical planning.[263,276–278] Furthermore, clinical bone reconstruction has largely benefited from 3D printing of customized implants, thanks to the advance of metal biomaterials printing technologies, such as electron beam melting [279] and selective laser melting.[280] However, when it comes to 3D bioprinting, cells and biomolecules come to the picture and makes it difficult to attain the required properties. Given challenging control of bioinks and 3D constructs, current state-of-art technology has been unable to robustly produce high aspect ratio structural features, i.e., those of complex organ shapes that require a large number of cells to be printed. This becomes of main concern particularly when it comes to irregular shapes with hanging features that require support structures to be printed. One example of such geometries are finely organized vascularization features that need to remain interconnected throughout the printed structure. Inefficient vascularization within the tissue implies the lack of oxygen delivery and nutrition diffusion. Tissue vascularization has a detrimental impact on the survival, integration, and function of any 3D construct that may be transplanted.[281] To circumvent such issues, attempts have been made to take advantage of patterned biomaterials, growth factors and coculture of printed cells with ECs, which leads to faster vascularization.[282] Other strategies of managing this issue have been the incorporation of oxygen releasing components within the bioink and suppressing the cellular metabolism.[283] In addition, using a sacrificial ink to template the vasculature architecture that can be later removed has been successfully addressed. 3D printing of removable materials with tubular structures to make an interconnected network for vascular cell culture has attracted attention[202] as a promising solution to tackle the limitation of vascularization.

On the other hand, low viscosity bioinks are difficult to remain in place, particularly when deposition-to-crosslinking time is long. Printing fidelity for such materials and geometries, therefore, need to be improved to enable fabricating well-vascularized tissue constructs. Furthermore, the interaction with the host tissue at the interface between the bioprinted construct and the target organ is currently not adequately addressed. Aside from the potential foreign body reactions and potential formation of scar tissue around the implanted structure, other risks of failure, such as local displacement or structural modes of deformation stemmed from repeated loads and viscoelastic permanent deformations have previously led to the rejection of the biomedical products.[284] Chemical and mechanical properties of bioinks and 3D bioprinted constructs vary overtime. Most of the performance evaluations in vitro and in vitro have been essentially performed in a limited time, thereby the lack of long-term data is a major concern when the clinical translation is contemplated. Further understanding is needed in the first place, to promote the integration between the 3D printed construct and the host tissue. This can be attained by engineering the chemistry of the material and functional groups present on the surface that may interact with the surrounding tissue for better integration. It is worth noting that despite successful results obtained in vitro and in vivo, the application of such engineered tissue grafts in the clinic may result in different adverse effects. Unfortunately, there is only a limited number of reports on in vivo experiments, particularly those employing large animal models and long-term follow-up mainly because of costly and time-consuming experiments. This signifies the need for undertaking a careful preclinical evaluation of both small and large animal models, conducting long-term studies and use intelligent evaluation and interpretation of accumulating data. This complexity has led to having different regulatory and approval procedures in different countries. Additionally, there exists a lack of standardized methodology for characterizing the responses to the biological stimulations.[173] From the industrial perspective, the benefit of 3D bioprinting must outweigh the current practice of biomedical solutions in order to push the products to the market. For instance, the regenerative role of 3D bioprinting should have specific attention, which is seriously lacking in the case of 3D printed implants. Therefore, it seems that there is a big demand for research on different aspects of 3D bioprinting, from bioink preparation and processing, all the way to preclinical animal testing and translation to the clinic.

7. Conclusions

The use of microfluidic-based 3D bioprinting is expected to enable the development of a broad range of functional tissues with many important applications in basic research, drug discovery, product testing, and ultimately in the clinic. Conceptually, it broadly expands the design space and ultimately tissue complexity as it enables us to have greater control over deposited bioinks and resulting structures in terms of size, composition, type of cells, and molecules used and programmed gradients. In addition, it offers more cell-friendly processing microenvironment as the printing systems are being designed

specifically for handling cells. The inherent characteristics of the approach and use of well-understood materials, such as PDMS and prototyping toolboxes including the use of 3D printing allows for the integration of valves, sensors, and continuous monitoring and control of the printing process. There have already been many reported examples of direct application of this technology to biofabrication of functional cell-laden fibers through wet spinning and recently 3D printed and viable tissue constructs. However, the applications of this technology are broad and still emerging as the field is still in the early stages of development. However, expected that over the next several years we will begin to see clinical success following the growing investment and research using in vivo studies of 3D bioprinted structures using these novel approaches. Ultimately, the development of advanced biomimetic 3D constructs will enable the treatment of a wide variety of tissue defects as well as directly contribute to organ repair and tissue regeneration.

Acknowledgements

This article is part of the Advanced Materials Technologies Hall of Fame article series, which recognizes the excellent contributions of leading researchers to the field of technology-related materials science. The authors acknowledge funding from the National Institutes of Health (EB021857-01A1, AR073135), Department of Defense: BiofabUSA Quick Start Project, the Natural Sciences and Engineering Research Council of Canada (NSERC: 50503-10243), and the Federal Economic Development Agency for Southern Ontario (FedDev Ontario: 809104). This study was supported by the National Science Centre – Poland (NCN) within the POLONEZ 3 fellowship number 2016/23/P/NZ1/03604 which has received funding from the European Union's Horizon 2020 research and innovation programme under the Marie Skłodowska-Curie grant agreement No. 665778 and the National Centre for Research and Development (STRATEGMED3/305813/2/NCBR/2017-BIONIC). This work was also financially supported by the Natural Science and Engineering Research Council of Canada, the Canada Research Chairs program, the Michael Smith Foundation for Health Research, and the Pacific Parkinson's Research Institute.

Conflict of Interest

The authors declare no conflict of interest.

Keywords

bioinks, biomimetic materials, bioprinting, microfluidics, tissue engineering

Received: November 22, 2019
Revised: February 19, 2020
Published online: May 26, 2020

[1] G. Rasperini, R. Acunzo, G. Pellegrini, G. Pagni, M. Tonetti, G. P. Pini Prato, P. Cortellini, *J. Clin. Periodontol.* **2018**, *45*, 1107.
[2] M. S. Tonetti, P. Cortellini, G. Pellegrini, M. Nieri, D. Bonaccini, M. Allegri, P. Bouchard, F. Cairo, G. Conforti, I. Fourmousis, F. Graziani, A. Guerrero, J. Halben, J. Malet, G. Rasperini, H. Topoll, H. Wachtel, B. Wallkamm, I. Zabalegui, O. Zuhr, *J. Clin. Periodontol.* **2018**, *45*, 78.
[3] B. J. Jank, L. Xiong, P. T. Moser, J. P. Guyette, X. Ren, C. L. Cetrulo, D. A. Leonard, L. Fernandez, S. P. Fagan, H. C. Ott, *Biomaterials* **2015**, *61*, 246.
[4] M. Takeo, T. Tsuji, *Curr. Opin. Genet. Dev.* **2018**, *52*, 42.
[5] P. Sanchez, *Cryobiology* **2015**, *71*, 177.
[6] W. C. Wilson, T. Boland, *Anat. Rec.* **2003**, *272A*, 491.
[7] T. Boland, V. Mironov, A. Gutowska, E. A. Roth, R. R. Markwald, *Anat. Rec.* **2003**, *272A*, 497.
[8] B. Dhariwala, E. Hunt, T. Boland, *Tissue Eng.* **2004**, *10*, 1316.
[9] I. T. Ozbolat, *Trends Biotechnol.* **2015**, *33*, 395.
[10] H.-W. Kang, S. J. Lee, I. K. Ko, C. Kengla, J. J. Yoo, A. Atala, *Nat. Biotechnol.* **2016**, *34*, 312.
[11] W. Zhu, X. Qu, J. Zhu, X. Ma, S. Patel, J. Liu, P. Wang, C. S. E. Lai, M. Gou, Y. Xu, K. Zhang, S. Chen, *Biomaterials* **2017**, *124*, 106.
[12] E. Y. S. Tan, W. Y. Yeong, *Int. J. Bioprint.* **2015**, *1*, 49.
[13] A. Panwar, L. P. Tan, A. Panwar, L. P. Tan, *Molecules* **2016**, *21*, 685.
[14] S. Sakai, K. Mochizuki, Y. Qu, M. Mail, M. Nakahata, M. Taya, *Biofabrication* **2018**, *10*, 045007.
[15] H.-W. Han, S.-H. Hsu, *Neural Regener. Res.* **2017**, *12*, 1595.
[16] G. Gao, A. F. Schilling, K. Hubbell, T. Yonezawa, D. Truong, Y. Hong, G. Dai, X. Cui, *Biotechnol. Lett.* **2015**, *37*, 2349.
[17] G. Gao, X. Cui, *Biotechnol. Lett.* **2016**, *38*, 203.
[18] A. Bsoul, S. Pan, E. Cretu, B. Stoeber, K. Walus, *Lab Chip* **2016**, *16*, 3351.
[19] A. Sorkio, L. Koch, L. Koivusalo, A. Deiwick, S. Miettinen, B. Chichkov, H. Skottman, *Biomaterials* **2018**, *171*, 57.
[20] E. Pagès, M. Rémy, V. Kériquel, M. M. Correa, B. Guillotin, F. Guillemot, *J. Nanotechnol. Eng. Med.* **2015**, *6*, 021006.
[21] S. Catros, V. Keriquel, J.-C. Fricain, F. Guillemot, *In Vivo and In Situ Biofabrication by Laser-Assisted Bioprinting*, Elsevier, Winston-Salem, USA **2015**.
[22] A. K. Miri, D. Nieto, L. Iglesias, H. Goodarzi Hosseinabadi, S. Maharjan, G. U. Ruiz-Esparza, P. Khoshakhlagh, A. Manbachi, M. R. Dokmeci, S. Chen, S. R. Shin, Y. S. Zhang, A. Khademhosseini, *Adv. Mater.* **2018**, *30*, 1800242.
[23] Z. Wang, H. Kumar, Z. Tian, X. Jin, J. F. Holzman, F. Menard, K. Kim, *ACS Appl. Mater. Interfaces* **2018**, *10*, 26859.
[24] Z. Wang, R. Abdulla, B. Parker, R. Samanipour, S. Ghosh, K. Kim, *Biofabrication* **2015**, *7*, 045009.
[25] E. N. Udofia, W. Zhou, in *Proc. of the 29th Annual Int. Solid Freeform Fabrication Symp. 2018: An Additive Manufacturing Conference* (Eds: D. L. Bourell, J. J. Beaman, R. H. Crawford, S. Fish, C. C. Seepersad), University of Texas at Austin, Austin, TX **2018**.
[26] L. Ning, X. Chen, *Biotechnol. J.* **2017**, *12*, 1600671.
[27] L. Aydın, A. Serdar Küçük, A. Halime Kenar, *Int. J. Appl. Math. Electron. Comput.* **2016**, *4*, 52.
[28] S. V Murphy, A. Atala, *Nat. Biotechnol.* **2014**, *32*, 773.
[29] T. D. Ngo, A. Kashani, G. Imbalzano, K. T. Q. Nguyen, D. Hui, *Composites, Part B* **2018**, *143*, 172.
[30] I. T. Ozbolat, Y Yu, *IEEE Trans. Biomed. Eng.* **2013**, *60*, 691.
[31] S. Derakhshanfar, R. Mbeleck, K. Xu, X. Zhang, W. Zhong, M. Xing, *Bioactive Mater.* **2018**, *3*, 144.
[32] P. Serra, A. Piqué, *Adv. Mater. Technol.* **2019**, *4*, 1800099.
[33] A. Skardal, A. Atala, *Ann. Biomed. Eng.* **2015**, *43*, 730.
[34] E. Breckenfeld, H. Kim, R. C. Y. Auyeung, A. Piqué, *J. Vis. Exp.* **2016**, e53728.
[35] F. Guillemot, A. Souquet, S. Catros, B. Guillotin, *Nanomedicine* **2010**, *5*, 507.
[36] F. Guillemot, A. Souquet, S. Catros, B. Guillotin, J. Lopez, M. Faucon, B. Pippenger, R. Bareille, M. Rémy, S. Bellance, P. Chabassier, J. C. Fricain, J. Amédée, *Acta Biomater.* **2010**, *6*, 2494.
[37] B. Guillotin, A. Souquet, S. Catros, M. Duocastella, B. Pippenger, S. Bellance, R. Bareille, M. Rémy, L. Bordenave, J. Amédée, F. Guillemot, *Biomaterials* **2010**, *31*, 7250.

[38] Y.-J. Seol, H.-W. Kang, S. J. Lee, A. Atala, J. J. Yoo, *Eur. J. Cardio-Thoracic Surg.* **2014**, *46*, 342.
[39] E. S. Bishop, S. Mostafa, M. Pakvasa, H. H. Luu, M. J. Lee, J. M. Wolf, G. A. Ameer, T.-C. He, R. R. Reid, *Genes Dis.* **2017**, *4*, 185.
[40] C. Khatiwala, R. Law, B. Shepherd, S. Dorfman, M. Csete, *Gene Ther. Regul.* **2012**, *07*, 1230004.
[41] M. Guvendiren, J. Molde, R. M. D. Soares, J. Kohn, *ACS Biomater. Sci. Eng.* **2016**, *2*, 1679.
[42] J. B. Hu, M. L. Tomov, J. W. Buikema, C. Chen, M. Mahmoudi, S. M. Wu, V. Serpooshan, *Appl. Phys. Rev.* **2018**, *5*, 041106.
[43] C. S. Ong, T. Fukunishi, H. Zhang, C. Y. Huang, A. Nashed, A. Blazeski, D. DiSilvestre, L. Vricella, J. Conte, L. Tung, G. F. Tomaselli, N. Hibino, *Sci. Rep.* **2017**, *7*, 4566.
[44] Z. Wang, S. J. Lee, H.-J. Cheng, J. J. Yoo, A. Atala, *Acta Biomater.* **2018**, *70*, 48.
[45] V. K. Lee, D. Y. Kim, H. Ngo, Y. Lee, L. Seo, S.-S. Yoo, P. A. Vincent, G. Dai, *Biomaterials* **2014**, *35*, 8092.
[46] P. Datta, B. Ayan, I. T. Ozbolat, *Acta Biomater.* **2017**, *51*, 1.
[47] V. K. Lee, A. M. Lanzi, H. Ngo, S.-S. Yoo, P. A. Vincent, G. Dai, N. Haygan, S.-S. Yoo, P. A. Vincent, G. Dai, *Cell Mol. Bioeng.* **2014**, *7*, 460.
[48] P. Mozetic, S. M. Giannitelli, M. Gori, M. Trombetta, A. Rainer, *J. Biomed. Mater. Res., Part A* **2017**, *105*, 2582.
[49] Y. Yu, Y. Zhang, I. T. Ozbolat, *J. Manuf. Sci. Eng.* **2014**, *136*, 061013.
[50] Y.-J. Choi, T. G. Kim, J. Jeong, H.-G. Yi, J. W. Park, W. Hwang, D.-W. Cho, *Adv. Healthcare Mater.* **2016**, *5*, 2636.
[51] J. A. Phillippi, E. Miller, L. Weiss, J. Huard, A. Waggoner, P. Campbell, *Stem Cells* **2008**, *26*, 127.
[52] X. Cui, K. Breitenkamp, M. G. Finn, M. Lotz, D. D. D'Lima, *Tissue Eng., Part A* **2012**, *18*, 1304.
[53] J. Kundu, J.-H. Shim, J. Jang, S.-W. Kim, D.-W. Cho, *J. Tissue Eng. Regener. Med.* **2015**, *9*, 1286.
[54] M. Müller, E. Öztürk, Ø. Arlov, P. Gatenholm, M. Zenobi-Wong, *Ann. Biomed. Eng.* **2017**, *45*, 210.
[55] C. Di Bella, A. Fosang, D. M. Donati, G. G. Wallace, P. F. M. Choong, *Front. Surg.* **2015**, *2*, 39.
[56] C. Stecco, *Functional Atlas of the Human Fascial System*, (Ed: W. Hammer), **2015**, p. 141.
[57] J. Watkins, *Pocket Podiatry: Functional Anatomy* (Ed: I. Mathieson), **2009**, p. 107.
[58] L. A. Smith, P. X. Ma, *Colloids Surf., B* **2004**, *39*, 125.
[59] L. G. Bracaglia, B. T. Smith, E. Watson, N. Arumugasaamy, A. G. Mikos, J. P. Fisher, *Acta Biomater.*. **2017**, *56*, 3.
[60] A. Hasan, A. Paul, N. E. Vrana, X. Zhao, A. Memic, Y.-S. Hwang, M. R. Dokmeci, A. Khademhosseini, *Biomaterials* **2014**, *35*, 7308.
[61] *Microfluidic Diagnostics* (Eds: G. Jenkins, C. D. Mansfield), Humana Press, Totowa, NJ **2013**.
[62] S. D. Minteer, *Microfluidic Techniques: Reviews and Protocols—Google Books*, Humana Press, New Jersey, NJ **2006**.
[63] A. Ebrahimi, W. Withayachumnankul, S. F. Al-Sarawi, D. Abbott, in *Microwave Microfluidic Sensor for Determination of Glucose Concentration in Water.*, IEEE, Lecce, Italy **2015**, pp.1–3.
[64] T. S. Kaminski, O. Scheler, P. Garstecki, *Lab Chip* **2016**, *16*, 2168.
[65] W. Engl, R. Backov, P. Panizza, *Curr. Opin. Colloid Interface Sci.* **2008**, *13*, 206.
[66] Y. Zheng, J. Nguyen, Y. Wei, Y. Sun, *Lab Chip* **2013**, *13*, 2464.
[67] R. Vadivelu, H. Kamble, M. Shiddiky, N.-T. Nguyen, R. K. Vadivelu, H. Kamble, M. J. A. Shiddiky, N.-T. Nguyen, *Micromachines* **2017**, *8*, 94.
[68] P. S. Dittrich, A. Manz, *Anal. Bioanal. Chem.* **2005**, *382*, 1771.
[69] F. Vollmer, S. Arnold, *Nat. Methods* **2008**, *5*, 591.
[70] I. E. Araci, S. R. Quake, *Lab Chip* **2012**, *12*, 2803.
[71] D. B. Weibel, M. Kruithof, S. Potenta, S. K. Sia, A. Lee, G. M. Whitesides, *Anal. Chem.* **2005**, *77*, 4726.
[72] R. H. Liu, J. Bonanno, J. Yang, R. Lenigk, P. Grodzinski, *Sens. Actuators, B.* **2004**, *98*, 328.
[73] G. Luka, A. Ahmadi, H. Najjaran, E. Alocilja, M. DeRosa, K. Wolthers, A. Malki, H. Aziz, A. Althani, M. Hoorfar, *Sensors* **2015**, *15*, 30011.
[74] D. Cogan, C. Fay, D. Boyle, C. Osborne, N. Kent, J. Cleary, D. Diamond, *Anal. Methods* **2015**, *7*, 5396.
[75] S. G. Yoon, H.-J. Koo, S. T. Chang, *ACS Appl. Mater. Interfaces* **2015**, *7*, 27562.
[76] O. Bonhomme, J. Leng, A. Colin, *Soft Matter* **2012**, *8*, 10641.
[77] B. R. Lee, K. H. Lee, E. Kang, D.-S. Kim, S.-H. Lee, *Biomicrofluidics* **2011**, *5*, 022208.
[78] C. H. Mun, J.-Y. Hwang, S.-H. Lee, *Tissue Eng. Regener. Med.* **2016**, *13*, 140.
[79] S. T. Beyer, A. Bsoul, A. Ahmadi, K. Walus, in *2013 Transducers Eurosensors XXVII 17th Int. Conf. Solid-State Sensors, Actuators Microsystems (TRANSDUCERS EUROSENSORS XXVII)*, IEEE, Piscataway, NJ **2013**, pp. 1206–1209.
[80] S. T. Beyer, T. Mohamed, K. Walus, in *The 17th Int. Conf. on Miniaturized Systems for Chemistry and Life Sciences (MicroTAS 2013)*, **2013**, pp. 176–178.
[81] M. Nie, P. Mistry, J. Yang, S. Takeuchi, in *2017 IEEE 30th Int. Conf. Micro Electro Mechanical Systems*, IEEE, Piscataway, NJ **2017**, pp. 589–591.
[82] M. Costantini, J. Idaszek, K. Szöke, J. Jaroszewicz, M. Dentini, A. Barbetta, J. E. Brinchmann, W. Święszkowski, *Biofabrication* **2016**, *8*, 035002.
[83] S. Ghorbanian, M. A. Qasaimeh, M. Akbari, A. Tamayol, D. Juncker, *Biomed. Microdevices* **2014**, *16*, 387.
[84] R. Attalla, E. Puersten, N. Jain, P. R. Selvaganapathy, *Biofabrication* **2018**, *11*, 015012.
[85] Q. Pi, S. Maharjan, X. Yan, X. Liu, B. Singh, A. M. van Genderen, F. Robledo-Padilla, R. Parra-Saldivar, N. Hu, W. Jia, C. Xu, J. Kang, S. Hassan, H. Cheng, X. Hou, A. Khademhosseini, Y. S. Zhang, *Adv. Mater.* **2018**, *30*, 1706913.
[86] W. Jia, P. S. Gungor-Ozkerim, Y. S. Zhang, K. Yue, K. Zhu, W. Liu, Q. Pi, B. Byambaa, M. R. Dokmeci, S. R. Shin, A. Khademhosseini, *Biomaterials* **2016**, *106*, 58.
[87] S. Ma, N. Mukherjee, *Adv. Biosyst.* **2018**, *2*, 1800119.
[88] Q. Gao, Z. Liu, Z. Lin, J. Qiu, Y. Liu, A. Liu, Y. Wang, M. Xiang, B. Chen, J. Fu, Y. He, *ACS Biomater. Sci. Eng.* **2017**, *3*, 399.
[89] E. Kang, Y. Y. Choi, S.-K. Chae, J.-H. Moon, J.-Y. Chang, S.-H. Lee, *Adv. Mater.* **2012**, *24*, 4271.
[90] M. E. Hoque, Y. L. Chuan, I. Pashby, *Biopolymers* **2012**, *97*, 83.
[91] I. T. Ozbolat, M. Hospodiuk, *Biomaterials* **2016**, *76*, 321.
[92] M. Costantini, C. Colosi, W. Święszkowski, A. Barbetta, W. Święszkowski, A. Barbetta, *Biofabrication* **2018**, *11*, 012001.
[93] K. Hölzl, S. Lin, L. Tytgat, S. Van Vlierberghe, L. Gu, A. Ovsianikov, *Biofabrication* **2016**, *8*, 032002.
[94] J. H. Y. Chung, S. Naficy, Z. Yue, R. Kapsa, A. Quigley, S. E. Moulton, G. G. Wallace, *Biomater. Sci.* **2013**, *1*, 763.
[95] J. Malda, J. Visser, F. P. Melchels, T. Jüngst, W. E. Hennink, W. J. A. Dhert, J. Groll, D. W. Hutmacher, *Adv. Mater.* **2013**, *25*, 5011.
[96] W. Liu, M. A. Heinrich, Y. Zhou, A. Akpek, N. Hu, X. Liu, X. Guan, Z. Zhong, X. Jin, A. Khademhosseini, Y. S. Zhang, *Adv. Healthcare Mater.* **2017**, *6*, 1601451.
[97] C. B. Highley, C. B. Rodell, J. A. Burdick, *Adv. Mater.* **2015**, *27*, 5075.
[98] M. Zhang, A. Vora, W. Han, R. J. Wojtecki, H. Maune, A. B. A. Le, L. E. Thompson, G. M. McClelland, F. Ribet, A. C. Engler, A. Nelson, *Macromolecules* **2015**, *48*, 6482.
[99] L. Ouyang, C. B. Highley, C. B. Rodell, W. Sun, J. A. Burdick, *ACS Biomater. Sci. Eng.* **2016**, *2*, 1743.

[100] K. Markstedt, A. Mantas, I. Tournier, H. Martínez Ávila, D. Hägg, P. Gatenholm, *Biomacromolecules* **2015**, *16*, 1489.
[101] L. K. Narayanan, P. Huebner, M. B. Fisher, J. T. Spang, B. Starly, R. A. Shirwaiker, *ACS Biomater. Sci. Eng.* **2016**, *2*, 1732.
[102] A. Kosik-Kozioł, M. Costantini, T. Bolek, K. Szöke, A. Barbetta, J. Brinchmann, W. Święszkowski, *Biofabrication* **2017**, *9*, 044105.
[103] A. Skardal, M. Devarasetty, H.-W. Kang, I. Mead, C. Bishop, T. Shupe, S. J. Lee, J. Jackson, J. Yoo, S. Soker, A. Atala, *Acta Biomater.* **2015**, *25*, 24.
[104] M. Kesti, M. Müller, J. Becher, M. Schnabelrauch, M. D'Este, D. Eglin, M. Zenobi-Wong, *Acta Biomater.* **2015**, *11*, 162.
[105] F. Maiullari, M. Costantini, M. Milan, V. Pace, M. Chirivì, S. Maiullari, A. Rainer, D. Baci, H. E.-S. Marei, D. Seliktar, C. Gargioli, C. Bearzi, R. Rizzi, *Sci. Rep.* **2018**, *8*, 13532.
[106] M. Costantini, S. Testa, P. Mozetic, A. Barbetta, C. Fuoco, E. Fornetti, F. Tamiro, S. |Bernardini, J. Jaroszewicz, W. Święszkowski, M. Trombetta, L. Castagnoli, D. Seliktar, P. Garstecki, G. Cesareni, S. Cannata, A. Rainer, C. Gargioli, *Biomaterials* **2017**, *131*, 98.
[107] Y. S. Zhang, A. Arneri, S. Bersini, S.-R. Shin, K. Zhu, Z. Goli-Malekabadi, J. Aleman, C. Colosi, F. Busignani, V. Dell'Erba, C. Bishop, T. Shupe, D. Demarchi, M. Moretti, M. Rasponi, M. R. Dokmeci, A. Atala, A. Khademhosseini, *Biomaterials* **2016**, *110*, 45.
[108] K. Zhu, S. R. Shin, T. van Kempen, Y.-C. Li, V. Ponraj, A. Nasajpour, S. Mandla, N. Hu, X. Liu, J. Leijten, Y.-D. Lin, M. A. Hussain, Y. S. Zhang, A. Tamayol, A. Khademhosseini, *Adv. Funct. Mater.* **2017**, *27*, 1605352.
[109] M. Yeo, J.-S. Lee, W. Chun, G. H. Kim, *Biomacromolecules* **2016**, *17*, 1365.
[110] X. Dai, L. Liu, J. Ouyang, X. Li, X. Zhang, Q. Lan, T. Xu, *Sci. Rep.* **2017**, *7*, 1457.
[111] C. Colosi, S. R. Shin, V. Manoharan, S. Massa, M. Costantini, A. Barbetta, M. R. Dokmeci, M. Dentini, A. Khademhosseini, *Adv. Mater.* **2016**, *28*, 677.
[112] C. Colosi, M. Costantini, A. Barbetta, M. Dentini, *Microfluidic Bioprinting of Heterogeneous 3D Tissue Constructs*, Humana Press, New York, NY **2017**.
[113] S. Khalil, W. Sun, *J. Biomech. Eng.* **2009**, *131*, 111002.
[114] A. Rajaram, D. Schreyer, D. Chen, *3D Print. Addit. Manuf.* **2014**, *1*, 194.
[115] N. Ashammakhi, A. Hasan, O. Kaarela, B. Byambaa, A. Sheikhi, A. K. Gaharwar, A. Khademhosseini, *Adv. Healthcare Mater.* **2019**, *8*, 1801048.
[116] Y. Jin, A. Compaan, T. Bhattacharjee, Y. Huang, *Biofabrication* **2016**, *8*, 025016.
[117] Y. Jin, W. Chai, Y. Huang, *Mater. Sci. Eng., C* **2017**, *80*, 313.
[118] T. Bhattacharjee, S. M. Zehnder, K. G. Rowe, S. Jain, R. M. Nixon, W. G. Sawyer, T. E. Angelini, *Sci. Adv.* **2015**, *1*, e1500655.
[119] S. Ostrovidov, V. Hosseini, S. Ahadian, T. Fujie, S. P. Parthiban, M. Ramalingam, H. Bae, H. Kaji, A. Khademhosseini, *Tissue Eng., Part B* **2014**, *20*, 403.
[120] S. Ostrovidov, S. Salehi, M. Costantini, K. Suthiwanich, M. Ebrahimi, R. B. Sadeghian, T. Fujie, X. Shi, S. Cannata, C. Gargioli, A. Tamayol, M. R. Dokmeci, G. Orive, W. Swieszkowski, A. Khademhosseini, *Small* **2019**, *15*, 1805530.
[121] R. Seyedmahmoud, B. Çelebi-Saltik, N. Barros, R. Nasiri, E. Banton, A. Shamloo, N. Ashammakhi, M. R. Dokmeci, S. Ahadian, *Micromachines* **2019**, *10*, 679.
[122] M. H. Mohammadi, R. Obregón, S. Ahadian, J. Ramón-Azcón, M. Radisic, *Curr. Pharm. Des.* **2017**, *23*, 2991.
[123] J. H. Kim, Y.-J. Seol, I. K. Ko, H.-W. Kang, Y. K. Lee, J. J. Yoo, A. Atala, S. J. Lee, *Sci. Rep.* **2018**, *8*, 12307.
[124] G. Vunjak-Novakovic, N. Tandon, A. Godier, R. Maidhof, A. Marsano, T. P. Martens, M. Radisic, *Tissue Eng., Part B* **2010**, *16*, 169.
[125] R. Gaetani, P. A. Doevendans, C. H. G. Metz, J. Alblas, E. Messina, A. Giacomello, J. P. G. Sluijter, *Biomaterials* **2012**, *33*, 1782.
[126] J. Jang, H.-J. Park, S.-W. Kim, H. Kim, J. Y. Park, S. J. Na, H. J. Kim, M. N. Park, S. H. Choi, S. H. Park, S. W. Kim, S.-M. Kwon, P.-J. Kim, D.-W. Cho, *Biomaterials* **2017**, *112*, 264.
[127] R. S. Udan, T. J. Vadakkan, M. E. Dickinson, *Development* **2013**, *140*, 4041.
[128] S. J. Paulsen, J. S. Miller, *Develop. Dyn.* **2015**, *244*, 629.
[129] C. Norotte, F. S. Marga, L. E. Niklason, G. Forgacs, *Biomaterials* **2009**, *30*, 5910.
[130] A. Skardal, J. Zhang, G. D. Prestwich, *Biomaterials* **2010**, *31*, 6173.
[131] Y. Zhang, Y. Yu, H. Chen, I. T. Ozbolat, *Biofabrication* **2013**, *5*, 025004.
[132] Y. Zhang, Y. Yu, I. T. Ozbolat, *J. Nanotechnol. Eng. Med.* **2013**, *4*, 20902.
[133] Q. Gao, Y. He, J. Fu, A. Liu, L. Ma, *Biomaterials* **2015**, *61*, 203.
[134] D. Zhu, X. Tong, P. Trinh, F. Yang, *Tissue Eng., Part A* **2018**, *24*, 1.
[135] J.-H. Shim, J.-S. Lee, J. Y. Kim, D.-W. Cho, J.-S. L. Jin-Hyung, S. Jong, Y. Kim, D.-W. Ch, *J. Micromech. Microeng.* **2012**, *22*, 085014.
[136] M. Kesti, C. Eberhardt, G. Pagliccia, D. Kenkel, D. Grande, A. Boss, M. Zenobi-Wong, *Adv. Funct. Mater.* **2015**, *25*, 7406.
[137] Y. Shi, T. L. Xing, H. B. Zhang, R. X. Yin, S. M. Yang, J. Wei, W. J. Zhang, *Biomed. Mater.* **2018**, *13*, 035008.
[138] P. Admane, A. C. Gupta, P. Jois, S. Roy, C. Chandrasekharan Lakshmanan, G. Kalsi, B. Bandyopadhyay, S. Ghosh, *Bioprinting* **2019**, *15*, e00051.
[139] A. M. Jorgensen, M. Varkey, A. Gorkun, C. Clouse, L. Xu, Z. Chou, S. V. Murphy, J. Molnar, S. J. Lee, J. J. Yoo, S. Soker, A. Atala, *Tissue Eng., Part A* **2020**, 10.1089/ten. tea.2019.0319.
[140] K. A. Homan, D. B. Kolesky, M. A. Skylar-Scott, J. Herrmann, H. Obuobi, A. Moisan, J. A. Lewis, *Sci. Rep.* **2016**, *6*, 34845.
[141] D. M. Kirchmajer, R. Gorkin III, M. in het Panhuis, *J. Mater. Chem. B* **2015**, *3*, 4105.
[142] A. I. Isayev, *Encyclopedia of Polymer Blends. Volume 2, Processing*, Wiley-VCH Verlag & Co. KGaA, Weinheim, Germany **2011**.
[143] J. K. Carrow, P. Kerativitayanan, M. K. Jaiswal, G. Lokhande, A. K. Gaharwar, in Essentials of 3D Biofabrication and Translation, (Eds: A Atala, J. J. Yoo) **2015**, 229.
[144] D. Chimene, K. K. Lennox, R. R. Kaunas, A. K. Gaharwar, *Ann. Biomed. Eng.* **2016**, *44*, 2090.
[145] E. Maréchal, *Comprehensive Polymer Science*, Pergamon Press, Oxford **1989**, p. 1.
[146] M. Müller, J. Becher, M. Schnabelrauch, M. Zenobi-Wong, *Biofabrication* **2015**, *7*, 035006.
[147] R. Suntornnond, E. Y. S. Tan, J. An, C. K. Chua, *Sci. Rep.* **2017**, *7*, 16902.
[148] E. Gioffredi, M. Boffito, S. Calzone, S. M. Giannitelli, A. Rainer, M. Trombetta, P. Mozetic, V. Chiono, *Proc. CIRP* **2016**, *49*, 125.
[149] E. Axpe, M. Oyen, *Int. J. Mol. Sci.* **2016**, *17*, 1976.
[150] S. Kyle, Z. M. Jessop, A. Al-Sabah, I. S. Whitaker, *Adv. Healthcare Mater.* **2017**, *6*, 1700264.
[151] A. G. Tabriz, M. A. Hermida, N. R. Leslie, W. Shu, *Biofabrication* **2015**, *7*, 045012.
[152] T. Jiang, J. G. Munguia-Lopez, S. Flores-Torres, J. Kort-Mascort, J. M. Kinsella, *Appl. Phys. Rev.* **2019**, *6*, 011310.
[153] Q. Wu, M. Maire, S. Lerouge, D. Therriault, M.-C. Heuzey, *Adv. Biosyst.* **2017**, *1*, 1700058.
[154] J. Zhang, B. J. Allardyce, R. Rajkhowa, Y. Zhao, R. J. Dilley, S. L. Redmond, X. Wang, X. Liu, *ACS Biomater. Sci. Eng.* **2018**, *4*, 3036.
[155] T. H. Barker, *Biomaterials* **2011**, *32*, 4211.
[156] R. C. Dutta, A. K. Dutta, *Biotechnol. Adv.* **2010**, *28*, 764.
[157] F. Rosso, A. Giordano, M. Barbarisi, A. Barbarisi, *J. Cell. Physiol.* **2004**, *199*, 174.
[158] B. Toprakhisar, A. Nadernezhad, E. Bakirci, N. Khani, G. A. Skvortsov, B. Koc, *Macromol. Biosci.* **2018**, *18*, 1800024.

[159] F. Pati, J. Jang, D.-H. Ha, S. Won Kim, J.-W. Rhie, J.-H. Shim, D.-H. Kim, D.-W. Cho, *Nat. Commun.* **2014**, *5*, 3935.
[160] J. A. Claudio-Rizo, J. Delgado, I. A. Quintero-Ortega, J. L. Mata-Mata, B. Mendoza-Novelo, *Hydrogels*, InTech, London **2018**.
[161] N. Ashammakhi, S. Ahadian, C. Xu, H. Ko, H. Montazerian, A. Khademhosseini, *Mater. Today Bio* **2019**, *1*, 100008.
[162] N. Cubo, M. Garcia, J. F. del Cañizo, D. Velasco, J. L. Jorcano, *Biofabrication* **2016**, *9*, 015006.
[163] T. K. Merceron, M. Burt, Y.-J. Seol, H.-W. Kang, S. J. Lee, J. J. Yoo, A. Atala, *Biofabrication* **2015**, *7*, 035003.
[164] J.-H. Shim, K.-M. Jang, S. K. Hahn, J. Y. Park, H. Jung, K. Oh, K. M. Park, J. Yeom, S. H. Park, S. W. Kim, J. H. Wang, K. Kim, D.-W. Cho, *Biofabrication* **2016**, *8*, 014102.
[165] H. Ashraf, B. Meer, R. Naz, A. Saeed, H. Sadia, U. Sajid, K. Nasir, Z. Aslam, P. Anwar, *Adv. Life Sci.* **2018**, *5*,143.
[166] A. Arslan-Yildiz, R. El Assal, P. Chen, S. Guven, F. Inci, U. Demirci, *Biofabrication* **2016**, *8*, 014103.
[167] F. Shahabipour, N. Ashammakhi, S. Bonakdar, R. K. Oskuee, M. A. Shokrgozar, H. Dehghani, A. Khademhosseini, S. Bonakdar, T. Hoffman, M. A. Shokrgozar, A. Khademhosseini, *Transl. Res.* **2019**, *216*, 57.
[168] S. Massa, M. A. Sakr, J. Seo, P. Bandaru, A. Arneri, S. Bersini, E. Zare-Eelanjegh, E. Jalilian, B.-H. Cha, S. Antona, A. Enrico, Y. Gao, S. Hassan, J. P. Acevedo, M. R. Dokmeci, Y. S. Zhang, A. Khademhosseini, S. R. Shin, *Biomicrofluidics* **2017**, *11*, 044109.
[169] H. Grover, C.-P. Spatarelu, K. De'De', S. Zhao, K. Yang, Y. Shrike Zhang, Z. Chen, *AIMS Cell Tissue Eng.* **2018**, *2*, 163.
[170] D. B. Kolesky, R. L. Truby, A. S. Gladman, T. A. Busbee, K. A. Homan, J. A. Lewis, *Adv. Mater.* **2014**, *26*, 3124.
[171] W. Liu, Y. S. Zhang, M. A. Heinrich, F. De Ferrari, H. L. Jang, S. M. Bakht, M. M. Alvarez, J. Yang, Y.-C. Li, G. T.-d. Santiago, A. K. Miri, K. Zhu, P. Khoshakhlagh, G. Prakash, H. Cheng, X. Guan, Z. Zhong, J. Ju, G. H. Zhu, X. Jin, S. R. Shin, M. R. Dokmeci, A. Khademhosseini, *Adv. Mater.* **2017**, *29*, 1604630.
[172] J. Idaszek, M. Costantini, T. A. Karlsen, J. Jaroszewicz, C. Colosi, S. Testa, E. Fornetti, S. Bernardini, M. Seta, K. Kasarełło, R. Wrzesień, S. Cannata, A. Barbetta, C. Gargioli, J. E. Brinchman, W. Święszkowski, *Biofabrication* **2019**, *11*, 044101.
[173] N. Tellisi, N. A. Ashammakhi, F. Billi, O. Kaarela, *J. Craniofacial Surg.* **2018**, *29*, 2363.
[174] G. M. Whitesides, *Nature* **2006**, *442*, 368.
[175] P. S. Dittrich, A. Manz, *Nat. Rev. Drug Discovery* **2006**, *5*, 210.
[176] A. Miri, E. Mostafavi, D. Khorsandi, S.-K. Hu, M. Malpica, A. Khademhosseini, *Biofabrication* **2019**, *11*, 042002.
[177] G. S. Ugolini, R. Visone, A. Redaelli, M. Moretti, M. Rasponi, *Adv. Healthcare Mater.* **2017**, *6*, 1601170.
[178] S. R. Shin, T. Kilic, Y. S. Zhang, H. Avci, N. Hu, D. Kim, C. Branco, J. Aleman, S. Massa, A. Silvestri, J. Kang, A. Desalvo, M. A. Hussaini, S.-K. Chae,, A. Polini, N. Bhise, M. A. Hussain, H. Lee, M. R. Dokmeci, A. Khademhossein, *Adv. Sci.* **2017**, *4*, 1600522.
[179] H. A. Stone, A. D. Stroock, A. Ajdari, *Annu. Rev. Fluid Mech.* **2004**, *36*, 381.
[180] L. R. Volpatti, A. K. Yetisen, *Trends Biotechnol.*. **2014**, *32*, 347.
[181] M. Angelozzi, M. Miotto, L. Penolazzi, S. Mazzitelli, T. Keane, S. F. Badylak, R. Piva, C. Nastruzzi, *Mater. Sci. Eng., C* **2015**, *56*, 141.
[182] J. Su, Y. Zheng, H. Wu, *Lab Chip* **2009**, *9*, 996.
[183] N. Raja, H. Yun, *J. Mater. Chem. B* **2016**, *4*, 4707.
[184] J. O. Hardin, T. J. Ober, A. D. Valentine, J. A. Lewis, *Adv. Mater.* **2015**, *27*, 3279.
[185] I. T. Ozbolat, H. Chen, Y. Yu, *Rob. Comput.-Integr. Manuf.* **2014**, *30*, 295.
[186] T. Kamperman, S. Henke, A. van den Berg, S. R. Shin, A. Tamayol, A. Khademhosseini, M. Karperien, J. Leijten, *Adv. Healthcare Mater.* **2017**, *6*, 1600913.
[187] P. R. Selvaganapathy, R. Attalla, *Proc. SPIE* **2016**, *9705*, 97050J.
[188] M. Yamada, R. Utoh, K. Ohashi, K. Tatsumi, M. Yamato, T. Okano, M. Seki, *Biomaterials* **2012**, *33*, 8304.
[189] E. Kang, S.-J. Shin, K. H. Lee, S.-H. Lee, *Lab Chip* **2010**, *10*, 1856.
[190] H. Onoe, T. Okitsu, A. Itou, M. Kato-negishi, R. Gojo, D. Kiriya, K. Sato, S. Miura, S. Iwanaga, K. Kuribayashi-shigetomi, Y. T. Matsunaga, Y. Shimoyama, S. Takeuchi, *Nat. Mater.* **2013**, *12*, 584.
[191] D. Kiriya, M. Ikeda, H. Onoe, M. Takinoue, H. Komatsu, Y. Shimoyama, I. Hamachi, S. Takeuchi, *Angew. Chem., Int. Ed.* **2012**, *51*, 1553.
[192] T. J. Ober, D. Foresti, J. A. Lewis, *Proc. Natl. Acad. Sci. USA* **2015**, *112*, 12293.
[193] T. Kamperman, S. Henke, B. Zoetebier, N. Ruiterkamp, R. Wang, B. Pouran, H. Weinans, M. Karperien, J. Leijten, *Mater. Biol. Med.* **2017**, *5*, 4835.
[194] P. S. Lienemann, T. Rossow, A. S. Mao, Q. Vallmajo-Martin, M. Ehrbar, D. J. Mooney, *Lab Chip* **2017**, *17*, 727.
[195] A. S. Mao, J. Shin, S. Utech, H. Wang, O. Uzun, W. Li, M. Cooper, Y. Hu, L. Zhang, D. A. Weitz, D. J. Mooney, *Nat. Mater.* **2017**, *16*, 236.
[196] N. E. Fedorovich, J. Alblas, J. R. de Wijn, W. E. Hennink, A. J. Verbout, W. J. A. Dhert, *Tissue Eng.* **2007**, *13*, 1905.
[197] Y. S. Zhang, Q. Pi, A. M. van Genderen, *J. Vis. Exp.* **2017**, *2017*, e55957.
[198] B. Byambaa, N. Annabi, K. Yue, G. Trujillo-de Santiago, M. M. Alvarez, W. Jia, M. Kazemzadeh-Narbat, S. R. Shin, A. Tamayol, A. Khademhosseini, *Adv. Healthcare Mater.* **2017**, *6*, 1700015.
[199] D. B. Kolesky, K. A. Homan, M. A. Skylar-Scott, J. A. Lewis, *Proc. Natl. Acad. Sci. USA* **2016**, *113*, 3179.
[200] W. Wu, A. DeConinck, J. A. Lewis, *Adv. Mater.* **2011**, *23*, H183.
[201] L. M. Bellan, S. P. Singh, P. W. Henderson, T. J. Porri, H. G. Craighead, J. A. Spector, *Soft Matter* **2009**, *5*, 1354.
[202] J. S. Miller, K. R. Stevens, M. T. Yang, B. M. Baker, D.-H. T. Nguyen, D. M. Cohen, E. Toro, A. A. Chen, P. A. Galie, X. Yu, R. Chaturvedi, S. N. Bhatia, C. S. Chen, *Nat. Mater.* **2012**, *11*, 768.
[203] L. E. Bertassoni, J. C. Cardoso, V. Manoharan, A. L. Cristino, N. S. Bhise, W. A. Araujo, P. Zorlutuna, N. E. Vrana, A. M. Ghaemmaghami, M. R. Dokmeci, A. Khademhosseini, *Biofabrication* **2014**, *6*, 024105.
[204] L. E. Bertassoni, M. Cecconi, V. Manoharan, M. Nikkhah, J. Hjortnaes, A. L. Cristino, G. Barabaschi, D. Demarchi, M. R. Dokmeci, Y. Yang, A. Khademhosseini, *Lab Chip* **2014**, *14*, 2202.
[205] W. Lee, V. Lee, S. Polio, P. Keegan, J.-H. Lee, K. Fischer, J.-K. Park, S.-S. Yoo, *Biotechnol. Bioeng.* **2010**, *105*, 1178.
[206] X. Ma, X. Qu, W. Zhu, Y.-S. Li, S. Yuan, H. Zhang, J. Liu, P. Wang, C. S. E. Lai, F. Zanella, G.-S. Feng, F. Sheikh, S. Chien, S. Chen, *Proc. Natl. Acad. Sci. USA* **2016**, *113*, 2206.
[207] S. J. wadsworth, S. Pan, T. Mohamed, S. Beyer, *Am. J. Respir. Crit. Care Med.* **2016**, *193*, A2837.
[208] S. Wadsworth, S. Beyer, S. Pan, T. Mohamed, presented at *Second Annual Tissue EngIneering, Biofabrication and 3D-Bioprinting Conf.*, Boston, MA, USA March **2016**.
[209] C. Dickman, V. Russo, S. Pan, E. Käpylä, S. Beyer, T. Mohamed, S. Wadsworth, presented at *Int. Conf. Biofabrication*, Würzburg, Germany October **2018**.
[210] D. Wei, J. Sun, J. Bolderson, M. Zhong, M. J. Dalby, M. Cusack, H. Yin, H. Fan, X. Zhang, *ACS Appl. Mater. Interfaces* **2017**, *9*, 14606.
[211] X. Liu, Y. Zuo, J. Sun, Z. Guo, H. Fan, X. Zhang, *Carbohydr. Polym.* **2017**, *178*, 8.
[212] X. Hou, Y. S. Zhang, G. T. Santiago, M. M. Alvarez, J. Ribas, S. J. Jonas, P. S. Weiss, A. M. Andrews, J. Aizenberg, A. Khademhosseini, *Nat. Rev. Mater.* **2017**, *2*, 17016.

[213] G. Kaushik, J. Leijten, A. Khademhosseini, *STEM CELLS* **2017**, *35*, 51.
[214] Y. S. Zhang, R. Oklu, M. R. Dokmeci, A. Khademhosseini, *Cold Spring Harbor Perspect. Med.* **2018**, *8*, a025718.
[215] S. Abbasalizadeh, M. R. Larijani, A. Samadian, H. Baharvand, *Tissue Eng., Part C* **2012**, *18*, 831.
[216] L. Adamo, O. Naveiras, P. L. Wenzel, S. McKinney-Freeman, P. J. Mack, J. Gracia-Sancho, A. Suchy-Dicey, M. Yoshimoto, M. W. Lensch, M. C. Yoder, G. García-Cardeña, G. Q. Daley, *Nature* **2009**, *459*, 1131.
[217] K. Yamamoto, T. Sokabe, T. Watabe, K. Miyazono, J. K. Yamashita, S. Obi, N. Ohura, A. Matsushita, A. Kamiya, J. Ando, *Am. J. Physiol.: Heart Circ. Physiol.* **2005**, *288*, H1915.
[218] L. Serex, A. Bertsch, P. Renaud, *Micromachines* **2018**, *9*, 86.
[219] R. Dong, Y. Liu, L. Mou, J. Deng, X. Jiang, *Adv. Mater.* **2019**, *31*, 1805033.
[220] J. Ma, Y. Wang, J. Liu, *RSC Adv.* **2018**, *8*, 21712.
[221] D. Kang, G. Ahn, D. Kim, H. W. Kang, S. Yun, W. S. Yun, J. H. Shim, S. Jin, *Biofabrication* **2018**, *10*, 035008.
[222] K. Zhu, N. Chen, X. Liu, X. Mu, W. Zhang, C. Wang, Y. S. Zhang, *Macromol. Biosci.* **2018**, *18*, 1800127.
[223] K. Kahin, Z. Khan, M. Albagami, S. Usman, S. Bahnshal, H. Alwazani, M. A. Majid, S. Rauf, C. Hauser, in *Microfluidics, BioMEMS, and Medical Microsystems XVII* (Eds: B. L. Gray, H. Becker), SPIE, San Francisco, California, USA **2019**.
[224] H. Montazerian, E. Davoodi, M. Asadi-Eydivand, J. Kadkhodapour, M. Solati-Hashjin, *Mater. Des.* **2017**, *126*, 98.
[225] A. Rahbari, H. Montazerian, E. Davoodi, S. Homayoonfar, *Comput. Methods Biomechan. Biomed. Eng.* **2017**, *20*, 231.
[226] H. Montazerian, M. Zhianmanesh, E. Davoodi, A. S. Milani, M. Hoorfar, *Mater. Des.* **2017**, *122*, 146.
[227] M. Zhianmanesh, M. Varmazyar, H. Montazerian, *ACS Biomater. Sci. Eng.* **2019**, *5*, 1228.
[228] H. Montazerian, M. G. A. Mohamed, M. M. Montazeri, S. Kheiri, A. S. Milani, K. Kim, M. Hoorfar, *Acta Biomater.*. **2019**, *96*, 149.
[229] S. M. Bittner, B. T. Smith, L. Diaz-Gomez, C. D. Hudgins, A. J. Melchiorri, D. W. Scott, J. P. Fisher, A. G. Mikos, *Acta Biomater.* **2019**, *90*, 37.
[230] J. Campbell, I. McGuinness, H. Wirz, A. Sharon, A. F. Sauer-Budge, *J. Nanotechnol. Eng. Med.* **2015**, *6*, 021005.
[231] J. Lee, K. E. Kim, S. Bang, I. Noh, C. Lee, *Int. J. Precis. Eng. Manuf.* **2017**, *18*, 605.
[232] E. Brouzes, M. Medkova, N. Savenelli, D. Marran, M. Twardowski, J. B. Hutchison, J. M. Rothberg, D. R. Link, N. Perrimon, M. L. Samuels, N. A. Clark, *Proc. Natl. Acad. Sci. USA* **2009**, *106*, 14195.
[233] M. Yamada, S. Sugaya, Y. Naganuma, M. Seki, *Soft Matter* **2012**, *8*, 3122.
[234] C. J. Hansen, R. Saksena, D. B. Kolesky, J. J. Vericella, S. J. Kranz, G. P. Muldowney, K. T. Christensen, J. A. Lewis, *Adv. Mater.* **2013**, *25*, 96.
[235] I. N. Aguilar, L. J. Smith, D. J. Olivos, T. M. G. Chu, M. A. Kacena, D. R. Wagner, *Bioprinting* **2019**, *15*, e00048.
[236] E. Davoodi, H. Fayazfar, F. Liravi, E. Jabari, E. Toyserkani, *Addit. Manuf.* **2020**, *32*, 101016.
[237] M. A. Heinrich, W. Liu, A. Jimenez, J. Yang, A. Akpek, X. Liu, Q. Pi, X. Mu, N. Hu, R. M. Schiffelers, J. Prakash, J. Xie, Y. S. Zhang, *Small* **2019**, *15*, 1805510.
[238] D. Cho, B. S. Kim, J. Jang, G. Gao, W. Han, N. K. Singh, *3D Bioprinting: Modeling In Vitro Tissues and Organs Using Tissue-Specific Bioinks*, Springer Nature, Switzerland AG **2019**.
[239] I. Matai, G. Kaur, A. Seyedsalehi, A. McClinton, C. T. Laurencin, *Biomaterials* **2020**, *226*, 119536.
[240] E. Abelseth, L. Abelseth, L. De la Vega, S. T. Beyer, S. J. Wadsworth, S. M. Willerth, *ACS Biomater. Sci. Eng.* **2019**, *5*, 234.
[241] T. Jiang, J. G. Munguia-Lopez, S. Flores-Torres, J. Kort-Mascort, J. M. Kinsella, *Appl. Phys. Rev.* **2019**, *6*, 011310.
[242] N. Chen, K. Zhu, Y. S. Zhang, S. Yan, T. Pan, M. Abudupataer, G. Yu, M. F. Alam, L. Wang, X. Sun, Y. Yu, C. Wang, W. Zhang, *ACS Appl. Mater. Interfaces* **2019**, *11*, 30585.
[243] S. Ji, M. Guvendiren, *Front. Bioeng. Biotechnol.* **2017**, *5*, 23.
[244] P. S. Gungor-Ozkerim, I. Inci, Y. S. Zhang, A. Khademhosseini, M. R. Dokmeci, *Biomater. Sci.* **2018**, *6*, 915.
[245] D. Ke, S. V. Murphy, *Tissue Eng., Part B* **2019**, *25*, 1.
[246] S. H. Oh, C. L. Ward, A. Atala, J. J. Yoo, B. S. Harrison, *Biomaterials* **2009**, *30*, 757.
[247] S. Khorshidi, A. Karkhaneh, S. Bonakdar, *J. Biomed. Mater. Res., Part A* **2020**, *108*, 136.
[248] H. W. Ooi, C. Mota, A. Tessa Ten Cate, A. Calore, L. Moroni, M. B. Baker, *Biomacromolecules* **2018**, *19*, 3390.
[249] A. Blaeser, D. F. Duarte Campos, U. Puster, W. Richtering, M. M. Stevens, H. Fischer, *Adv. Healthcare Mater.* **2016**, *5*, 326.
[250] A. McCormack, C. B. Highley, N. R. Leslie, F. P. W. Melchels, *Trends Biotechnol.* **2020**, *38*, 584.
[251] L. de la Vega, D. A. Rosas Gómez, E. Abelseth, L. Abelseth, V. Allisson da Silva, S. Willerth, L. de la Vega, D. A. Rosas Gómez, E. Abelseth, L. Abelseth, V. Allisson da Silva, S. M. Willerth, *Appl. Sci.* **2018**, *8*, 2414.
[252] E. Masaeli, V. Forster, S. Picaud, F. Karamali, M.-H. Nasr-Esfahani, C. A. Marquette, *Biofabrication* **2019**, *12*, 025006.
[253] D. A. Gregory, P. Kumar, A. Jimenez-Franco, Y. Zhang, Y. Zhang, S. J. Ebbens, X. Zhao, *J. Vis. Exp.* **2019**, *2019*, e59030.
[254] D. Takagi, W. Lin, T. Matsumoto, H. Yaginuma, N. Hemmi, S. Hatada, M. Seo, *Int. J. Bioprint.* **2019**, *5*, 27.
[255] O. Kérourédan, D. Hakobyan, M. Rémy, S. Ziane, N. Dusserre, J. C. Fricain, S. Delmond, N. B. Thébaud, R. Devillard, *Biofabrication* **2019**, *11*, 045002.
[256] C. Mandrycky, Z. Wang, K. Kim, D. H. Kim, *Biotechnol. Adv.* **2016**, *34*, 422.
[257] R. Attalla, C. Ling, P. Selvaganapathy, *Biomed. Microdevices* **2016**, *18*, 17.
[258] K. Fetah, P. Tebon, M. J. Goudie, J. Eichenbaum, L. Ren, N. Barros, R. Nasiri, S. Ahadian, N. Ashammakhi, M. R. Dokmeci, A. Khademhosseini, *Prog. Biomed. Eng.* **2019**, *1*, 012001.
[259] A. Dick, B. Bhandari, S. Prakash, *Meat Science.* **2019**, *153*, 35.
[260] N. Ashammakhi, O. Kaarela, P. Ferretti, *J. Craniofac. Surg.* **2018**, *29*, 1.
[261] N. Ashammakhi, S. Ahadian, F. Zengjie, K. Suthiwanich, F. Lorestani, G. Orive, S. Ostrovidov, A. Khademhosseini, *Biotechnol. J.* **2018**, *13*, 1800148.
[262] Y. Lu, A. A. Aimetti, R. Langer, Z. Gu, *Nat. Rev. Mater.* **2017**, *2*, 16075.
[263] I. Pountos, N. Tellisi, N. Ashammakhi, *3D Bioprinting in Medicine*, Springer International Publishing, Cham **2019**.
[264] W.-C. Yan, P. Davoodi, S. Vijayavenkataraman, Y. Tian, W. C. Ng, J. Y. H. Fuh, K. S. Robinson, C.-H. Wang, *Adv. Drug Delivery Rev.* **2018**, *132*, 270.
[265] E. Abelseth, L. Abelseth, L. De la Vega, S. T. Beyer, S. J. Wadsworth, S. M. Willerth, *ACS Biomater. Sci. Eng.* **2019**, *5*, 234.
[266] P. Mostafalu, G. Kiaee, G. Giatsidis, A. Khalilpour, M. Nabavinia, M. R. Dokmeci, S. Sonkusale, D. P. Orgill, A. Tamayol, A. Khademhosseini, *Adv. Funct. Mater.* **2017**, *27*, 1702399.
[267] A. Tamayol, A. Hassani Najafabadi, P. Mostafalu, A. K. Yetisen, M. Commotto, M. Aldhahri, M. S. Abdel-wahab, Z. I. Najafabadi, S. Latifi, M. Akbari, N. Annabi, S. H. Yun, A. Memic, M. R. Dokmeci, A. Khademhosseini, *Sci. Rep.* **2017**, *7*, 9220.
[268] E. Davoodi, H. Montazerian, R. Haghniaz, A. Rashidi, S. Ahadian, A. Sheikhi, J. Chen, A. Khademhosseini, A. S. Milani, M. Hoorfar, E. Toyserkani, *ACS Nano* **2020**, *14*, 1520.

[269] H. Montazerian, A. Rashidi, A. Dalili, H. Najjaran, A. S. Milani, M. Hoorfar, *Small* **2019**, *15*, 1804991.
[270] N. Ashammakhi, M. A. Darabi, I. Pountos, *J. Craniof. Surg.* **2019**, *30*, 623.
[271] N. Fekete, M. T. Rojewski, D. Fürst, L. Kreja, A. Ignatius, J. Dausend, H. Schrezenmeier, *PLoS One* **2012**, *7*, e43255.
[272] D. Kami, K. Watakabe, M. Yamazaki-Inoue, K. Minami, T. Kitani, Y. Itakura, M. Toyoda, T. Sakurai, A. Umezawa, S. Gojo, *BMC Biotechnol.* **2013**, *13*, 102.
[273] J. Lee, H.-A. Kao, S. Yang, *Proc. CIRP* **2014**, *16*, 3.
[274] C. Thuemmler, C. Bai, *Health 4.0: How Virtualization and Big Data Are Revolutionizing Healthcare*, Springer International Publishing, Switzerland **2017**.
[275] C. Thuemmler, C. Bai, *Health 4.0: How Virtualization Big Data Are Revolutionizing Healthcare*, Springer International Publishing, Cham **2017**.
[276] S. Singare, Q. Lian, W. Ping Wang, J. Wang, Y. Liu, D. Li, B. Lu, *Rapid Prototyping J.* **2009**, *15*, 19.
[277] P. A. Webb, *J. Med. Eng. Technol.* **2000**, *24*, 149.
[278] M. Robiony, I. Salvo, F. Costa, N. Zerman, M. Bazzocchi, F. Toso, C. Bandera, S. Filippi, M. Felice, M. Politi, *J. Oral Maxillofac. Surg.* **2007**, *65*, 1198.
[279] J. Parthasarathy, B. Starly, S. Raman, A. Christensen, *J. Mech. Behav. Biomed. Mater.* **2010**, *3*, 249.
[280] J. Matena, S. Petersen, M. Gieseke, A. Kampmann, M. Teske, M. Beyerbach, H. Escobar, H. Haferkamp, N.-C. Gellrich, I. Nolte, *Int. J. Mol. Sci.* **2015**, *16*, 7478.
[281] S. Correia Carreira, R. Begum, A. W. Perriman, *Adv. Healthcare Mater.* **2019**, 1900554.
[282] M. D. Sarker, S. Naghieh, N. K. Sharma, L. Ning, X. Chen, *J. Healthcare Eng.* **2019**, *2019*, 1.
[283] N. Ashammakhi, M. A. Darabi, N. S. Kehr, A. Erdem, S. Hu, M. R. Dokmeci, A. S. Nasr, A. Khademhosseini, *Biomacromolecules* **2019**, *21*, 56.
[284] M. Shemesh, R. Asher, E. Zylberberg, F. Guilak, E. Linder-Ganz, J. J. Elsner, *J. Mech. Behav. Biomed. Mater.* **2014**, *29*, 42.
[285] T. Takei, S. Sakai, H. Ijima, K. Kawakami, *Biotechnol. J.* **2006**, *1*, 1014.
[286] S.-J. Shin, J.-Y. Park, J.-Y. Lee, H. Park, Y.-D. Park, K.-B. Lee, C.-M. Whang, S.-H. Lee, *Langmuir* **2007**, *23*, 9104.
[287] S. Sugiura, T. Oda, Y. Aoyagi, M. Satake, N. Ohkohchi, M. Nakajima, *Lab Chip* **2008**, *8*, 1255.
[288] R. Chang, J. Nam, W. Sun, *Tissue Eng., Part C* **2008**, *14*, 157.
[289] K. H. Lee, S. J. Shin, Y. Park, S.-H. Lee, *Small* **2009**, *5*, 1264.
[290] S. Mazzitelli, L. Capretto, D. Carugo, X. Zhang, R. Piva, C. Nastruzzi, *Lab Chip* **2011**, *11*, 1776.
[291] E. Kang, G. S. Jeong, Y. Y. Choi, K. H. Lee, A. Khademhosseini, S. Lee, *Nat. Mater.* **2011**, *10*, 877.
[292] Y. Yu, Y. Zhang, J. A. Martin, I. T. Ozbolat, *J. Biomech. Eng.* **2013**, *135*, 91011.
[293] F. Dolati, Y. Yu, Y. Zhang, A. M. De Jesus, E. A. Sander, I. T. Ozbolat, A. M. De Jesus, E. A. Sander, I. T. Ozbolat, *Nanotechnology* **2014**, *25*, 145101.
[294] T. Sun, Q. Huang, Q. Shi, H. Wang, X. Liu, M. Seki, · M Nakajima, T. Fukuda, *Microfluid. Nanofluid.* **2015**, *19*, 1169.
[295] S. Li, Y. Liu, Y. Li, C. Liu, Y. Sun, Q. Hu, *Biomicrofluidics* **2016**, *10*, 064104.
[296] W. Liu, Z. Zhong, N. Hu, Y. Zhou, L. Maggio, A. K. Miri, A. Fragasso, X. Jin, A. Khademhosseini, Y. S. Zhang, *Biofabrication* **2018**, *10*, 024102.
[297] A. Kumachev, J. Greener, E. Tumarkin, E. Eiser, P. W. Zandstra, E. Kumacheva, *Biomaterials* **2011**, *32*, 1477.
[298] Y. Ma, M. P. Neubauer, J. Thiele, A. Fery, W. T. S. Huck, *Biomater. Sci.* **2014**, *2*, 1661.
[299] X. Zhao, S. Liu, L. Yildirimer, H. Zhao, R. Ding, H. Wang, W. Cui, D. Weitz, *Adv. Funct. Mater.* **2016**, *26*, 2809.
[300] W. Yang, H. Yu, G. Li, Y. Wang, L. Liu, *Small* **2017**, *13*, 1602769.